Czech Technical University in Prague
Faculty of Mechanical Engineering

Department of Automotive, Combustion Engine and Railway Engineering
Study program: Master of Automotive Engineering
Field of study: Advanced Powertrains

GASEOUS FUEL INJECTION FOR ENGINE WITH A SCAVENGED PRE-CHAMBER

Author : Kamane Akshay
Supervisor : Ing. Jiří Vávra, Ph.D
Tutor : Ing. Zbyněk Syrovátka
Year : 2019

Disclaimer

I hereby declare the following thesis is my independent work and to the best of knowledge. I have only used the document listed in the attachments. It contains no materials previously published or written by any other person

In Prague: 19/08/2019 _____

Akshay Kamane

Acknowledgment

Firstly, I would like to express my sincere gratitude to my thesis supervisor Ing. Jiří Vávra, Ph.D. for giving me this opportunity. His guidance, continuous support, knowledge has motivated me throughout my thesis and helped me achieve my goals. Besides my supervisor, I am grateful to Ing. Zbyněk Syrovátka who guided me whenever needed. A special thanks to Ing Marcel Divis for his consultations and Ing Vit Dolecek for all the help in GT-Power. And finally, I would like to thank my family and friends for all the love, support and care throughout my studies.

Akshay Kamane

ABSTRACT

This thesis deals with the design of a gaseous fuel injection system for a single-cylinder 4-stroke engine with a scavenged pre-chamber for metering the fuel supply through the ball check valve into the pre-chamber. Various simulations were performed on the fuel injection system model in GT-POWER to study the behavior of the check valve and predict the mechanical parameters of the valve for different operating conditions. The GT Power model was calibrated for the flow rate of various conditions based on the provided experimental data from the gas engine for a light-duty truck. A sensitivity analysis was carried out for the mechanical parameter to examine the effect of it on the output flow rate.

Later on, the fuel injection model was coupled with a model of single-cylinder research engine of the size of a small automotive engine model to study the performance of the check valve at full load condition of engine for larger speed range. Finally, the eigenfrequencies were determined for the check valve and the helical spring from the valve using VTDESIGN workbench in GT SUITE to assess the resonance conditions.

Keywords: Check Valve, Pre-chamber, GT SUITE, Natural gas, Natural frequency.

Contents

Nomenclature 3

1. Introduction 4

2. Literature review 6

2.1 Lean-Burn Combustion 6

2.2 Alternative Ignition system 7

2.2.1 Laser-Induced Ignition 7

2.2.2 Diesel Pilot Injection 8

2.2.3 Pre chamber Ignition 9

3.Experimental Setup 11

3.1 Experimental Engine 11

3.2 Pre-chamber Design 12

3.3 Ball Check Valve 14

4. GT POWER Model 16

4.1 Fuel Injection System Model 16

4.2 Methodology used for the simulation 18

4.3 Sensitivity analysis of the mechanical parameters of the check valve 18

4.3.1 Effect of Spring Stiffness on the flow rate 19

4.3.2 Effect of the Spring preload on the flow rate 20

4.4 Simulation and Results 22

4.4.1 Engine in a stationary state 22

4.4.2 Unsteady-state Engine conditions 25

4.4.3 Thermal drift in pressure measurement 36

4.5 Summary and comparison of the results 39

5. Single Cylinder Research Engine 41
5.1 Pre-chamber design for high-speed research engine 41
5.2 GT-Power part 42
5.3 Full load condition simulation and results 43
6 Modal analysis of the Check Valve 48
6.1 Natural frequencies of the spring 49
Summary and Conclusion 51
Future Scope of the thesis 54
References 55
List of Figures 58
List of tables 60
List of files attached in CD 61
List of attachments 62

Nomenclature

η_{ith}	Indicated thermal efficiency
ω_e	Excitation frequency in rad/sec
f_e	Excitation frequency in Hertz(Hz)
k_s	Spring Stiffness
w_n	Natural frequency in rad/sec
w_n	Natural frequency in Hertz(Hz)
BDC	Bottom Dead Center
C	Celcius
CFD	Computational fluid dynamics
CH4	Methane
CNG	Compressed Natural Gas
CO2	Carbon dioxide
CR	Compression ratio
DC	Direct current
DOE	Design of experiments
ECU	Electronic control unit
GHG	Greenhouse gases
HC	Hydrocarbons
K	Kelvin
LPG	Liquified natural gas
N2	Nitrogen
N2O	Nitrous oxide
Nox	Oxides of Nitrogen
RPM	Revolution per minute
TDC	Top dead center
UHC	Unburnt Hydrocarbons
VFR	Volume flow rate
VGT	Variable geometry turbine

1. Introduction

The transportation system is one of the most important aspects of modern society, one would hardly imagine life without it. But with all the benefits it provides to us there are few major drawbacks to it which trigger us to think and innovate the technology. In the last few decades with rapid growth in population, the demand for use of automotive vehicles has tremendously increased all around the world. For years, gasoline and diesel were the primary fuel used in the automotive industry. The challenge with the use of these fuel for the operation is its high emissions after the combustion, although with the ongoing research, engineers and scientists around the world have been successful in reducing the emissions but the results are not very promising especially looking at the current climatic changes around the world and the number of humans affected by it. [1]

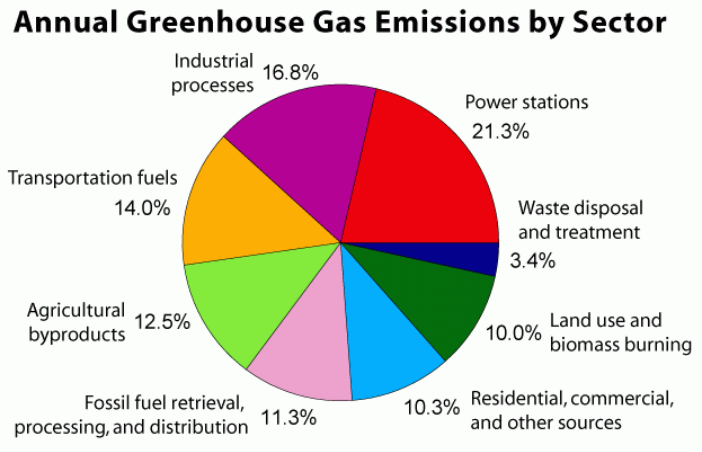

Figure 1 Green House Gases Emissions by sector [2]

Figure 1 shows the Greenhouse gases (GHG) emissions by various sector and it is seen that the transportation sector contributes to 14 % of the total greenhouse gas emissions. The internal combustion engine is the major contributor within the transportation sector, this is mainly due to high emissions of CO_2 gas caused by the combustion of the fuel. Along with CO_2, methane (CH_4), nitrous oxide (N_2O) and water vapor (H_2O) are also emitted which are greenhouse gases. Besides these gases, the diesel engine also emits particulate matter which is carcinogenic and might cause asthma, respiratory diseases, and lung cancer. Due to the above reasons, Natural gas is considered to be an alternative fuel.

Natural gas is made up of HC and primarily consists of CH_4, it is not only found in fossil fuel reserves but also can be produced with alternative waste. It is available in two forms of compressed natural gas (CNG) and liquified natural gas (LNG).

Natural gas, when operated in a lean air-fuel mixture offers various advantages [3]. Due to lower in-cylinder temperature as compared to lambda=1 operations, the heat losses are minimized and it also tends to low NOx production and emissions [4]. Also, Natural gas has a high octane number which helps to mitigate knock and enable high load operations. But the lean limit for combustion of the Natural gas is restricted by the capability of the ignition system to ignite the fuel-air lean mixture reliably [5]. To overcome this limitation pre-chamber type ignition is preferred. It is a simplified solution that requires fewer engine modifications and is less complex.

The fuel in the pre-chamber can be injected in many ways like with the help of fuel injectors [6]. Even though we get precise fuel control with help of injector a separate control system is required for it and it needs modifications in the cylinder head which makes it expensive. The other solution is to have a separate fuel injection system to the pre-chamber. The fuel enters the pre-chamber through a drilled passage with a built-in miniature check valve. The principle of working of the check valve is the differential pressure between upstream and downstream of the check valve. Check valves are simple, inexpensive and they operate automatically.

The scope of the thesis is to study the behavior of the ball check valve used for the current experimental setup for a light-duty truck engine tested up to 2400 rpm with the help of simulation results. The results will also help us monitor the opening and closing of the ball during the engine operation which is not possible experimentally and also allows us to meter the fuel passing through it. Further, the fuel injection model will be simulated for a larger speed range for a small automotive size engine model to see the performance of the check valve at higher operating speed.

Based on the results obtained from the studies, it will be assessed that if the ball check valve is solely sufficient to deliver the fuel as required to the pre-chamber without any external control or it might need some additional controllers. Since, the check valve is a simple spring-mass system, Modal analysis of the valve will be done to check for the resonance condition which is important while operating at high speed.

2. Literature review

The current available CNG engines are based on the SI engine with some modifications to improve and attain gasoline-like performance. The modifications involve the use of a high compression ratio as compared to the SI engine [7] due to the high octane rating of Natural gas, to reduce losses in volumetric efficiency fuel is directly injected in the engine. Increased boost pressure and variable valve actuation are also implemented.

Engine with such modification fails to take maximum advantage of properties of natural gas. The reason is the limitation of maximum peak in-cylinder pressure and operations at the stoichiometric ratio mainly due to emissions. This adds to the use of a catalytic converter to reduce emissions. However natural gas-operated in lean mixture offers a wide range of benefits which are discussed below.

2.1 Lean-Burn Combustion

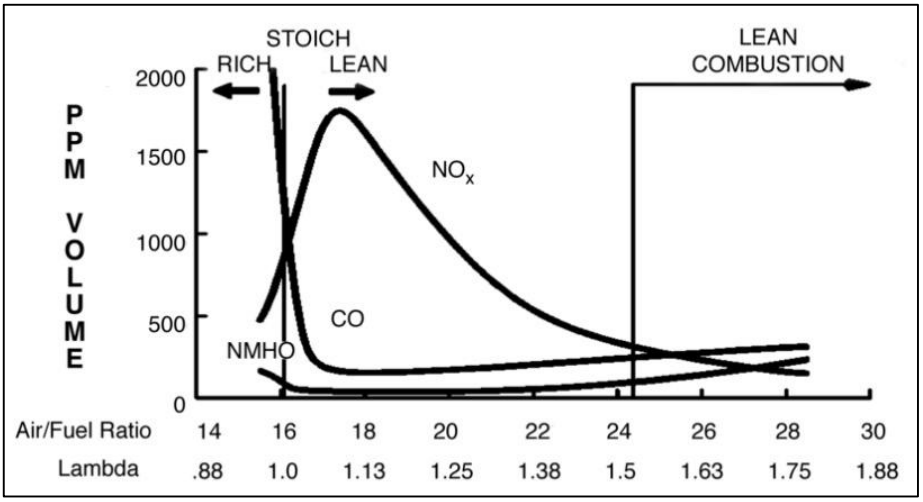

Figure 2 Emissions versus air/fuel ratio [4]

It is seen in figure 2, engines when operated in a lean mixture, tend to have very low emissions. Since, high temperature is one of the catalysts in NO_x production, when operated in a lean mixture the peak in-cylinder temperature is reduced resulting in lower NO_x emissions [9] and the overall heat losses are also decreased. Additional air in the lean mixture increases the specific heat ratio which in results increases the thermal efficiency. This is called the Lean Burn concept.

$$\eta_{ith} = 1 - \frac{1}{r_c^{\gamma-1}}$$

Where

η_{ith}= Indicated thermal efficiency

r_c = Compression ratio

γ = Specific Heat Ratio

In addition to this, lean burn combustion also helps to mitigate knock allowing the use of a high compression ratio which enables high load operations. The fuel consumption is also affected, such operation allows the engine to run at less throttle with the same power output thus resulting in lower fuel consumption.

Despite all the advantages, there are few limitations in using a lean mixture. The ignition energy required to reliably combust the fuel-air mixture is very high. If the energy is low it leads to a low burning rate and lowers flame speed which might cause misfire and results in high unburnt hydrocarbon(UHC) emissions. Therefore lean limit of the mixture is restricted by the capability of the ignition system to ignite the fuel-air mixture. To overcome the above limitation following alternative ignition system can be used: [10]

a. Laser-Induced Ignition
b. Diesel Pilot Injection
c. Pre-chamber type ignition

2.2 Alternative Ignition system

2.2.1 Laser-Induced Ignition

As the demand for high ignition energy to ignite the ultra-lean fuel-air mixture conventional spark plug is not efficient. Increased spark energy creates a negative impact thus affecting the durability of the spark plug and effectiveness in transmitting the energy. [11]

Laser ignition improves the ignition system durability, reduces the maintenance and increases engine combustion performance. As compared to conventional spark plug the point of ignition of the laser plug can be positioned at a distance which helps eliminates heat flame quenching in spark plugs. Laser-induced spark can discharge a high amount of energy instantaneously which helps in rising temperature and pressure quickly. This

extreme local condition helps in reducing the induction time which results in the rapid breaking of the hydrocarbon bonds meaning less ignition delay.

In spite of the above advantage, laser-induced ignition cannot be used in the mobile application, since the laser system is not fully developed and it would to difficult to implement it.

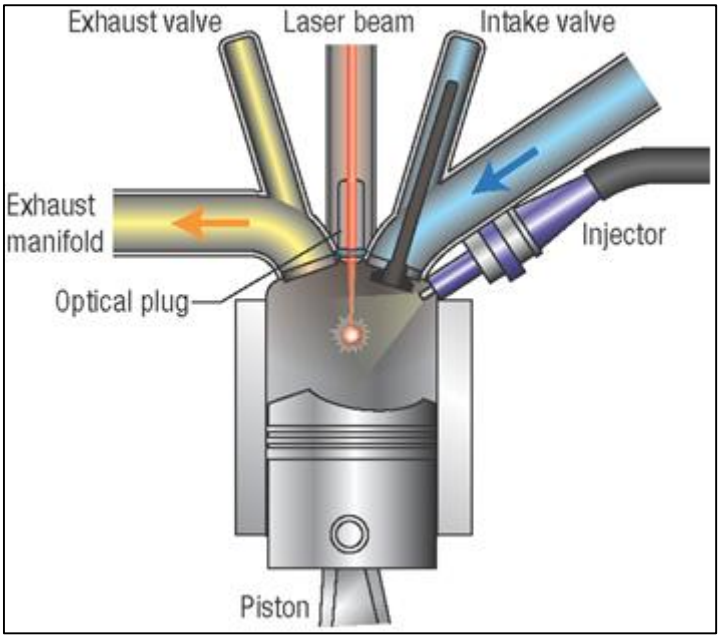

Figure 3 Laser-Induced Ignition [12]

2.2.2 Diesel Pilot Injection

The principle of pilot injection is to inject a small amount of fuel during the compression stroke to have high cylinder pressure at the end of compression stroke which will reduce the ignition delay for the main injection by generating energy for the combustion. [13] [10]

The ignition delay is defined as the time interval between the start of injection and the start of combustion. Both physical and chemical process must take place before the fraction of chemical energy of the injected fuel is released. The physical process mainly involves atomization, vaporization, and mixing of fuel. On the other hand, chemical processes are a pre-combustion reaction between a fuel, air and residual gases which lead to autoignition. The main purpose of the pilot injection is to reduce the delay during the chemical process to reduce the overall ignition time.

Diesel engine pilot injection has been implemented to some extent but only for the stationary applications, the main reason is due to ease of handling of two different fuel subsystems and limitations in space.

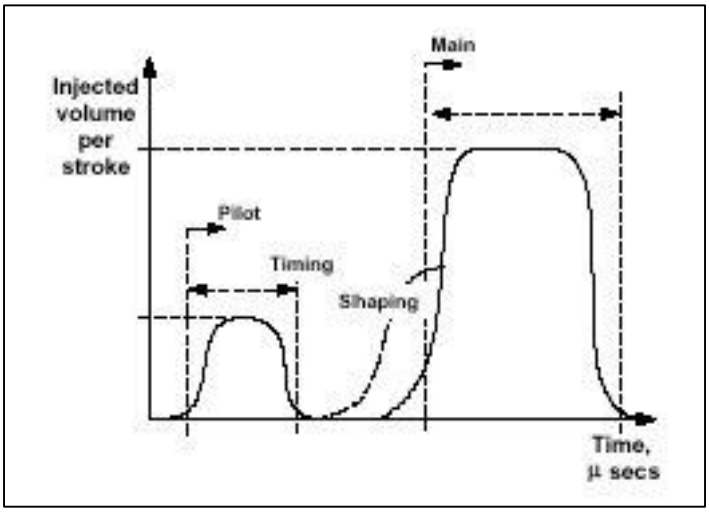

Figure 4 Pilot Injection [14]

2.2.3 Pre chamber Ignition

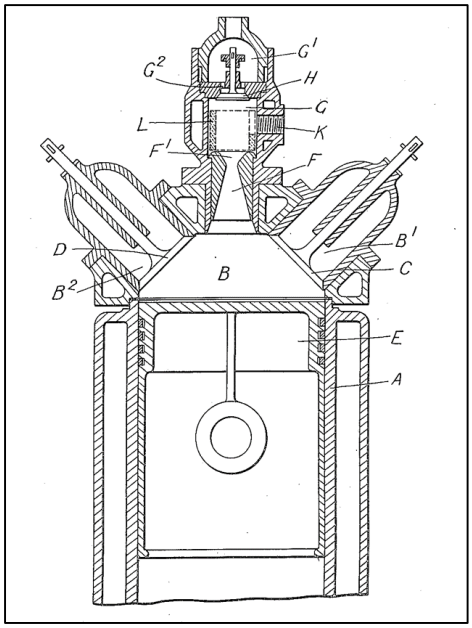

Figure 5 First pre-chamber design by Riccardo

[15] [10] Figure 5 shows the first pre-chamber design developed by Riccardo [16]. It has 3 valves, Valve D is the main intake valve allowing air to flow to the combustion chamber whereas mixture of fuel and air is introduced in pre-chamber through Valve H. The power output of the engine was governed by controlling the fuel

and air mixture quantity introduced in the pre-chamber leaving mass flow through main valve unchanged, hence reducing throttling losses.

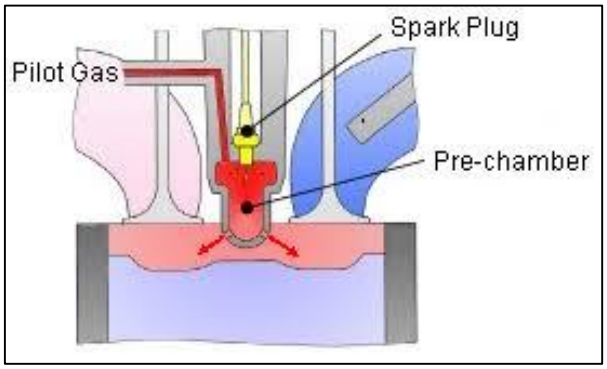

Figure 6 Working of the pre-chamber engine [17]

The pre-chamber can function as passive (without injection of gas) or scavenged (with the supply of gas), although passive pre-chamber is not considered for this study and its application. The main chamber can be supplied with a lean fuel-air mixture or only air depending on the application. Pre-chamber generally is filled with a rich mixture, during the compression stroke, the lean fuel-air mixture or air moves up in the pre-chamber to form an ignitable and slightly rich mixture. The mixture thus ignited in the pre-chamber with the help of high voltage spark produces a flame that comes out of the pre-chamber as a jet through holes into the main chamber thus resulting in the combustion of the remaining mixture.

A pre-chamber ignition system offers a simplified solution and is less complex compared to other ignition technologies. It also requires fewer engine modifications. An extremely lean homogeneous mixture can be burned with pre-chamber technology at a high combustion rate. Due to its various advantages, it has been a scope of research recently and this technology is also adapted for the current engine set up.

3.Experimental Setup

3.1 Experimental Engine

The initial experiments for the single-cylinder engine were conducted at the Czech Technical university laboratory at the Josef Bozek Research Centre for vehicles of sustainable mobility. The experimental setup was designed and developed by the predecessor and all the modifications done in-house.

The engine used for the setup is a 4-cylinder 4-stroke light duty truck engine. The engine was converted into a single-cylinder arrangement for the experiments by deactivating the other three cylinders. The deactivation was done by closing the intake and exhaust runners with the help of metal plates. Figure 7 shows the scheme of the arrangement of the engine, red lines indicate the closing of the intake and exhaust runner with metal plates so operates engine as a single-cylinder [18]

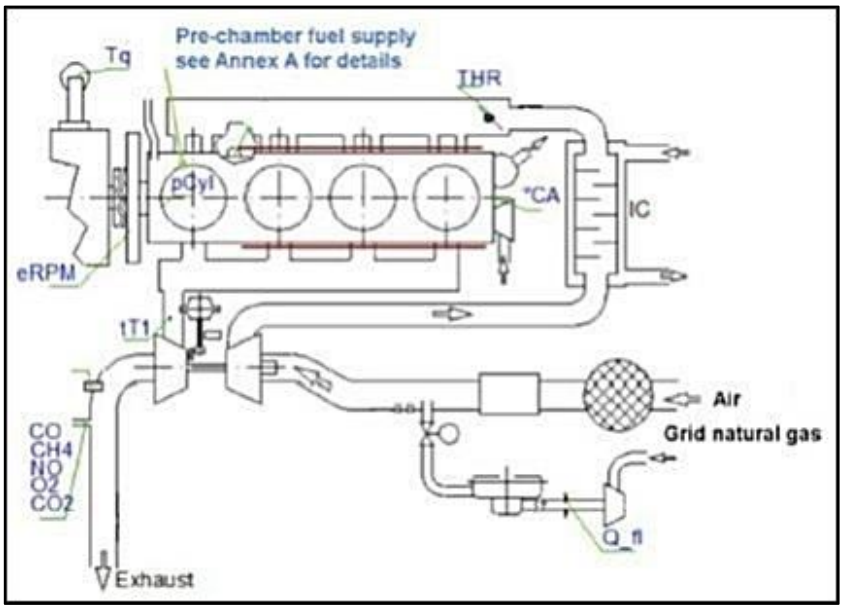

Figure 7 Scheme of current test engine layout

The main engine parameters in the original SI engine arrangement is listed in Table 1. The engine is turbocharged with an intercooler with a compression ratio of 12. The turbocharger model is CZ-C14 with VGT controlled by the ECU. It has a central mixing unit for feeding gaseous fuel in the compressor. There is a separate arrangement for injecting the gaseous fuel to the pre-chamber and is shown in the attachment C. By the use of conventional oxygen sensor output signal as feedback, it is possible to operate with closed-loop lambda control or manually control the fuel flow. A conventional throttle valve which is located downstream of the intercooler is actuated by a stepper

motor controlling the mixture inflow. A capacitive ignition system allows independent varying the spark timing. A field-programmable gate array developed by the predecessor controls the ECU and help to actuates all the actuators and sensors. The figure above shows the placement of all the sensors

No of cylinder	4
Bore/Stroke	102/120 mm
Displacement	3.94 dm3
Compression Ratio	12
Valves/cylinder	4
EVO/EVC	122/373 CA after firing TDC
IVO/IVC	342/595 CA after firing TDC

Table 1 Main parameters of the Engine

3.2 Pre-chamber Design

The cylinder head of one cylinder was modified so as to install the developed scavenged pre-chamber design as shown in figure 8. [19]

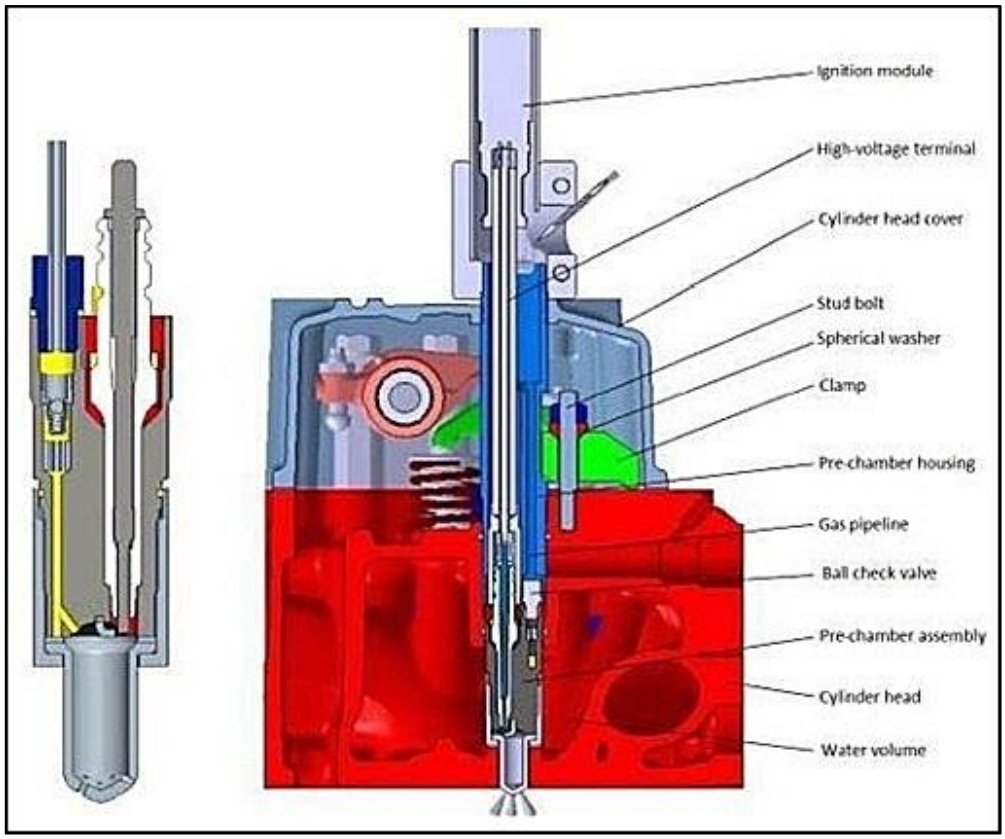

Figure 8 Pre-chamber Module Setup(left) and Cross-section of the cylinder head with pre-chamber assembly(right)

Pre-chamber parameters	
Volume	4.1 cm3
The fraction of compressed volume	4.6 %
CR with Pre-chamber	12.00:1
No of holes	12
Hole diameter	1.2

Table 2 Pre-chamber parameters [3]

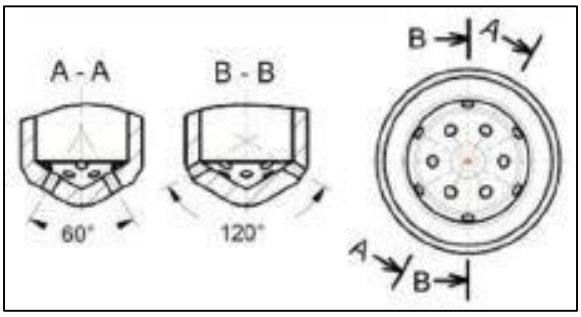

Figure 9 Pre-chamber geometry [18]

The pre-chamber design was designed in a modular way that allows modifications in size, geometry, and orifices. The gaseous fuel is injected into the pre-chamber through gas pipelines passing through the check valve as shown in figure 8. The schematic fuel supply system into the pre-chamber is presented in Attachment C. The laboratory is equipped with a compressed natural gas (CNG) line with gas pressure up to 200 bar. A pressure regulator is used to regulate the pressure to approximately 3 bar. Omega mass flow meter OMEGA FMA2610A controls and measures the fuel flow rate. Average volumetric flow rate can be visually inspected by a rotameter.

The pre-chamber is cylindrical and filling it with fresh gaseous fuel depends on the difference between instantaneous pre-chamber pressure and fuel supply pressure due to the presence of a check valve. Therefore this arrangement allows us to control the level of scavenging with the help of the mass flow controller. The fuel pressure should be adjusted in such a way that fuel flow starts at the end of the exhaust stroke and continues until the entire intake stroke to maximize the scavenging of pre-chamber from the residual gas.

During the compression, the ultra-lean mixture moves up into the pre-chamber to form a combustible mixture in the pre-chamber. The ideally stoichiometric or slightly

rich mixture should be present in the pre-chamber to ignite the mixture with the help of spark plug. Standard spark plug (brisk CR10YS) with a 0.5 mm spark gap was used.

Besides the spark plug and the fuel line in the pre-chamber, an uncooled AVL GH15D pressure transducer is also installed. The installation of the miniature transducer allows a crank angle resolved pressure measurement in the pre-chamber simultaneously with pressure measurement in the main chamber with another miniature uncooled pressure transducer ie AVL GU13Z-24. The in-house developed acquisition software and an angle calculator system complied in a National Instrument LabVIEW helps in recording signal at high speed. Later this pressure signal is amplified using two-channel Kistler charger amplifiers. This pressure signals from the pre-chamber are used as the boundary conditions for the simulations in GT Suite for fuel injection system model.

3.3 Ball Check Valve

The check valve is a type of non-return valve which allows the fluid flow in one specific direction and prevents the reverse flow. It is a simple ball and spring arrangement as shown in figure 10. The valves are compatible with hydraulic fluids, brake fluids, fuels, and oils. Check valves are generally very simple and inexpensive and they work automatically without external control. [20]

Lee Check check valve 558 series is used. The diameter of the ball is 2.1 mm and the seat diameter is 1.8 mm. The maximum possible displacement of the ball is 1.022 mm. The direction of the flow depends on the positioning of the ball.

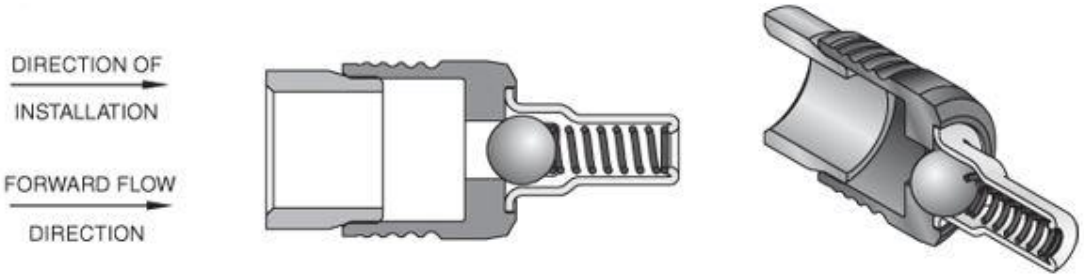

Figure 10 Ball check valve LEE 558 series forward flow

The opening and closing of the check valve are depended upon the differential pressure between upstream and downstream of the ball also termed as the cracking pressure. Cracking pressure is a function of spring stiffness and spring preloading. These parameters directly affect the performance of the valve thus the effect of varying

spring stiffness and preloading on the flow rate is studied and discussed in the further section.

The mechanical properties of the valve-like spring stiffness and spring preload are calculated from the simulation. With the help of these parameters, further studies will be conducted where the behavior of the check valve will be monitored when the research engine single-cylinder model will be simulated for a larger speed range.

Due to less knowledge and high sensitivity of the check valve, it is quite complicated to predict the exact values of the mechanical parameters. A methodology discussed in the further section has been adapted to estimate the parameters. From the obtained parameters, we can study the dynamics of the valve as well as carry out the modal analysis of the valve to determine the eigenfrequencies of the valve. Due to insufficient data, we have to depend on the simulation results to know the values of the mechanical parameters of the valve.

The installation instructions of the check valve are specified in the Lee installation manuals. It uses the insert principle to eliminate the need for threads and o-rings. Different valves have different installation forces. Further details of the check valve can be seen in attachment B.

4. GT POWER Model

A GT POWER model of the fuel injection system was designed to study the behavior of the ball check valve. A detailed yet simplified model was designed based on the provided geometric CAD data. The main focus was to study the performance of the ball valve since it directly affects the flow rate. The mechanical properties of the check valve, spring stiffness and preloading were the unknown parameters, due to insufficient data the exact values were missing. Therefore the model was tuned to find the best fits of these parameters to achieve approximately the same the flow rate that was measured during experiments. Hence we were dependent on the simulated results to know these mechanical parameters, the degree of accuracy cannot be specified. The model was simulated with different cases like steady-state and unsteady conditions with boundary conditions varying respectively.

The chapter has the following parts:

i. Modeling of the fuel injection system into the pre-chamber and setting up the model as per provided data and given conditions.
ii. Simulating the model for different conditions to study and understand the behavior of the model.
iii. Calibrating the model for the different conditions with experimental data provided from the engine tests to find out the mechanical parameters of the ball valve and comparing the results.
iv. Sensitivity analysis of the mechanical parameters of the check valve for studying the effect on the output flow rate.

4.1 Fuel Injection System Model

The GT Power model of the fuel injection system to deliver the fuel to the pre-chamber is seen in Attachment D.

The laboratory setup of the fueling system is seen in figure 11. The highlighted section of the system was considered to develop the GT Power model for the fuel injection system since it is assumed that the pressure losses in Rotameter are negligible. The pressure transducer is placed in pressure damping vessel (pNG5), the main purpose of this vessel is to reduce the pressure oscillations from the system if present especially from the fuel coming from the CNG cylinders, this means a constant value of pressure is sensed by the transducer which is considered as input boundary condition for the model. An end environment object represents the state of fuel in the pressure damping vessel (pNG5)

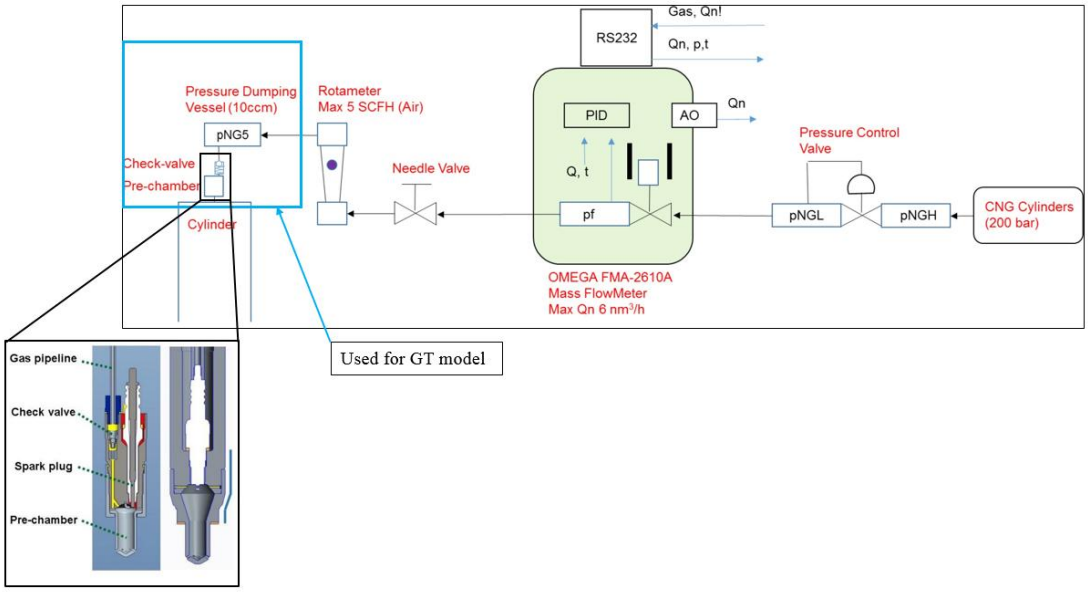

Figure 11 Laboratory fuel supply setup

Another end environment object characterizes the pre-chamber condition during the operation and boundary condition for the model are the instantaneous pressure and temperature profile in the pre-chamber which is sensed by a miniature pressure transducer positioned in the pre-chamber. A mechanical model consisting of a mass, spring is coupled with the flow model which simulates the mechanical properties of the ball valve. Although there is no physical damper present in the ball valve, a damper object is connected in the model to damp the vibrations and converged the results faster. The gas pipeline and capillary are modeled based on provided geometric CAD data.

The run setup and other parameters are set up similar to engine experimental condition. The following are the parameters from the case setup which can be changed by the user for different operation testing.

Parameters	Unit	Description
Input Pressure	Bar	The absolute pressure in the pressure damping vessel (pNG5)
Input Temperature	K	The temperature of the fuel in the pressure damping vessel (pNG5)
Input Fuel gas		Different fuel gas was used for the experiment for different operation and it can be changed in the Initial condition of input end environment.
Output Pressure	bar	Instantaneous pressure profile with respect to crank angle in the pre-chamber
Output Temperature	K	Instantaneous temperature profile with respect to crank angle in the pre-chamber

Engine speed	RPM	Engine operating speed
Lambda		Air excess

Table 3 Parameter that can be changed in the GT Power model

4.2 Methodology used for the simulation

As mentioned earlier due to the insufficient data about the check valve, the mechanical parameters of the valve which are spring stiffness and preloading are unknown. The model is simulated to find the approximate value of the parameters in order to have the same output volumetric flow rate flowing through the ball valve as measured by the OMEGA mass flow meter. In achieving so the following steps were taken during the simulation to get the results.

i. Setting up the model with the boundary condition and other parameters similar to engine experimental conditions.
ii. Simulating the model with initial values of the mechanical parameters and comparing the result with the experimental data for a single case.
iii. Running the Design Of Experiment(DOE) [21] set up for the range of the mechanical parameters based on the previous results.
iv. Trying to find the best fit of the mechanical parameters to achieve approximately similar flow rate within specified tolerances.
v. Re-run the model with selected parameters for all the cases and comparing the results with experimental data.
vi. Analyzing the model and plotting out the results.

4.3 Sensitivity analysis of the mechanical parameters of the check valve

As highlighted before the mechanical parameters of the check valve will be estimated from the simulation results. But before proceeding further, it was necessary to understand the effect of the variation of the mechanical parameters on the fuel flow rate passing through the valve. Hence, a sensitivity analysis is carried out to study the effect with the changing parameters

The fuel injection model from GT-power [Attachment D] was set up with a boundary condition identical to the experimental engine. The model was simulated at 1200 rpm engine speed. The output boundary condition was the instantaneous pressure profile recorded by the pressure transducer during the experiments. The operating gas

used for the simulation was natural gas with 98.4% methane with a standard density of 0.7175 Kg/m3 at 0^{o}C and atmospheric pressure. The injection pressure was set to 1.22 bar. The model was simulated to study the individual effect of the mechanical parameter on the flow rate keeping the other parameter constant.

4.3.1 Effect of Spring Stiffness on the flow rate

This study will help understand the effect of varying spring stiffness on the flow rate. The model was simulated with spring stiffness varying from 0.3-0.7 N/mm and constant preload of 0,7.5 and 15.5 kPa. The boundary condition was kept as mentioned above and the model was simulated. The plot in figure 12 shows the results of the flow rate with respect to spring stiffness.

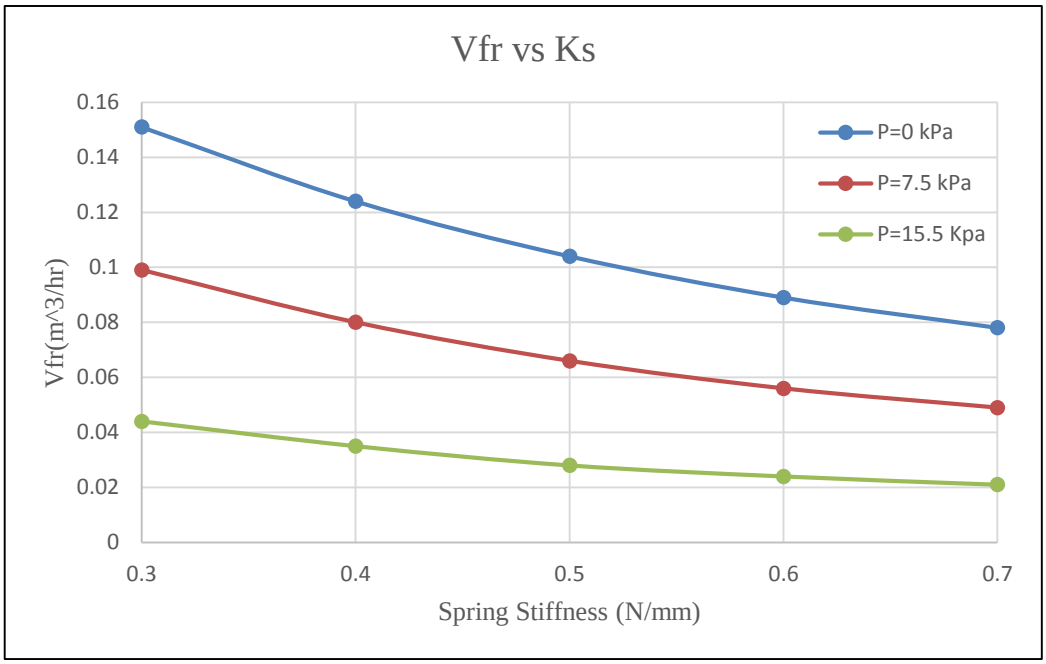

Figure 12 Standard Volumetric flow rate (m^3/hr) versus Spring Stiffness(N/mm)

It is observed from the above plot for spring stiffness of 0.3 N/mm and at zero preload, the maximum flow rate is achieved, however at the same preload as the spring stiffness increases the flow rate decreases. At the preload of 7.5 kPa and 15.5 kPa, similar trends were observed. At the spring stiffness of 0.7 N/mm and preload of 15.5 kPa the flow rate a minimum flow rate of 0.02 m^3/hr was seen. This indicates that at the constant preload as the spring stiffness decreases the flow rate increases, which

means the fuel injection system will deliver a slightly high amount of fuel to the pre-chamber under normal operating condition.

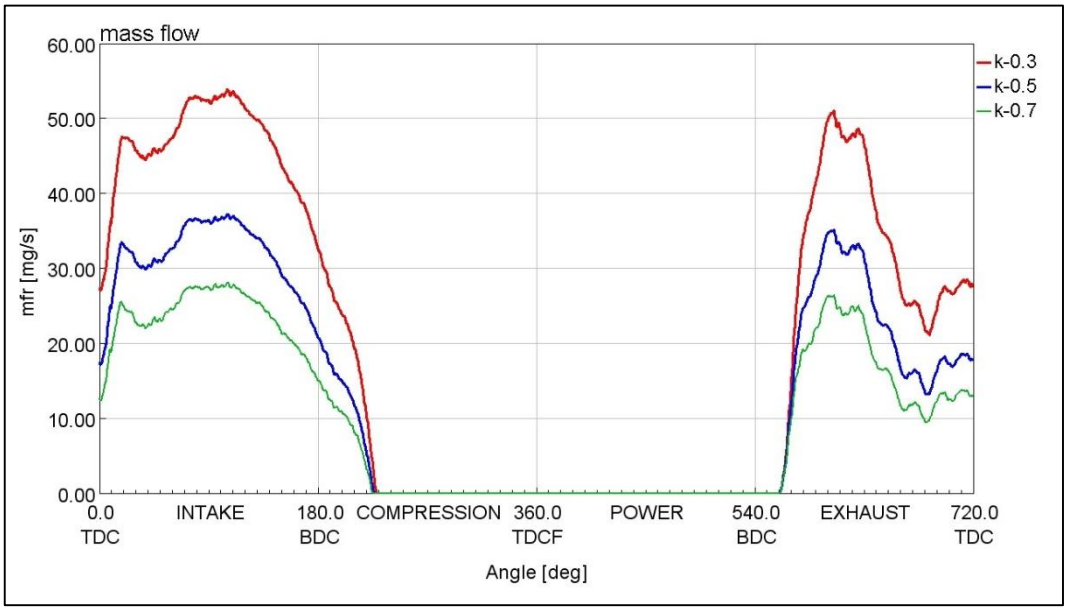

Figure 13 Instantaneous mass flow profile (mg/sec) Ks=0.3 vs 0.5 vs 0.7

The plot in figure 13 shows the instantaneous mass flow profile of the fuel passing through the check valve at 7.5 kPa and varying spring stiffness of 0.3,0.5 and 0.7 N/mm. Fuel flow to the pre-chamber is seen during the exhaust stroke and it increases as the spring stiffness decreases, which means the fuel losses per cycle will be higher since this fuel delivered to the pre-chamber during the exhaust event doesn't participate in the main combustion event and might affect the unburnt hydrocarbon emissions.

The check valve opens and closes at the same degree of the cycle. Since the valve opening and closing is governed by the cracking pressure of the valve this proves the cracking pressure is not affected by the spring stiffness.

4.3.2 Effect of the Spring preload on the flow rate

This section helps us to understand the effect of the changes in the flow rate with varying preload of the spring. The model was simulated with preloading ranging from 0 to 15.5 kPa and at constant spring stiffness of 0.3, 0.4 and 0.5 N/mm.

The model was set to similar boundary conditions as pervious case and results were obtained. The plot in figure 14 shows the relation of the flow rate with respect to spring preload.

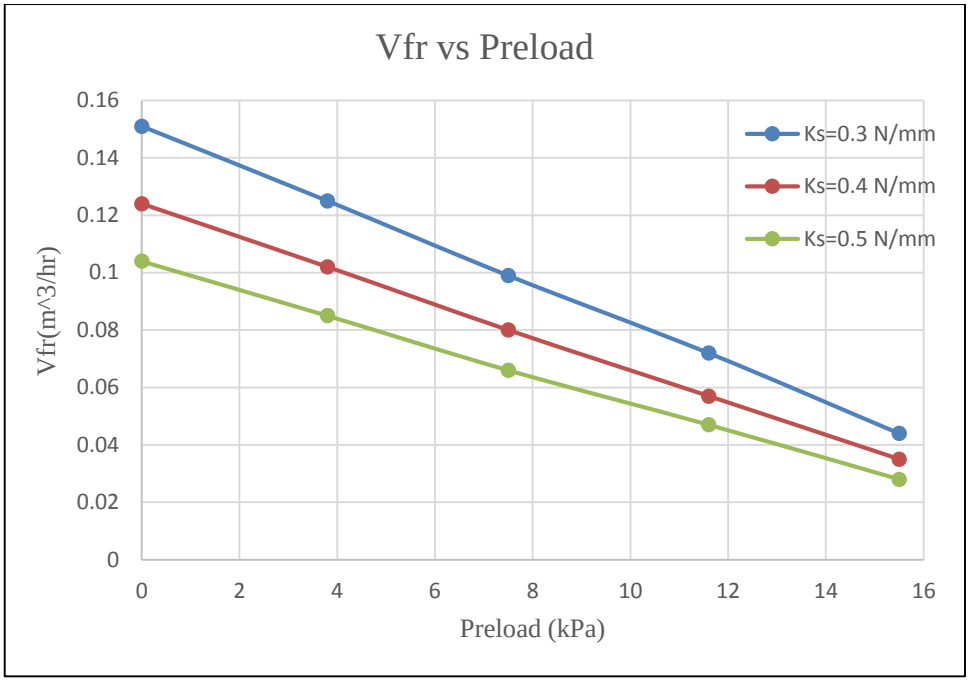

Figure 14 Standard Volumetric flow rate (m^3/hr) versus Spring preload(kPa)

It is observed that there is a linear variation of the flow rate with respect to the spring preload. As the preload increase, the overall flow rate decreases. The maximum flow rate is seen at zero spring preload and lower spring stiffness of 0.3 N/mm. For the same spring stiffness of 0.3 N/mm as the preloading is increased the flow rate drops drastically. But as the spring gets stiffer and at spring stiffness of 0.7 N/mm as the preload varies the flow rate changes gradually.

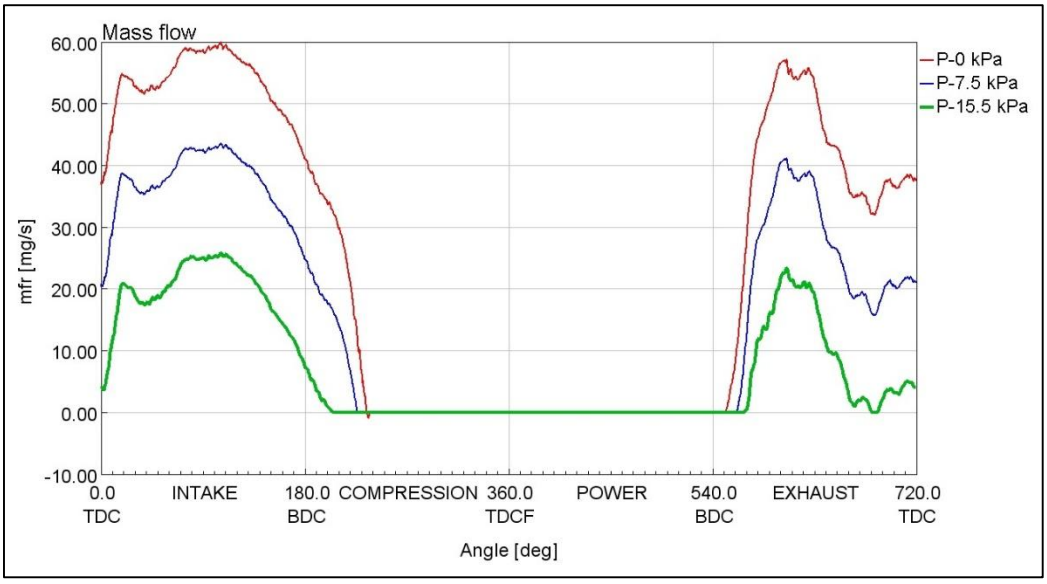

Figure 15 Instantaneous mass flow profile (mg/sec) - Preload= 0 vs 7.5 vs 15.5 kPa

The plot in figure 15 shows the instantaneous mass flow profile of the fuel through the check valve at 0.4 N/mm spring stiffness and varying preload. At the same engine operating conditions the flow rate increases quite significantly on both intake and exhaust side as preload decreases. Also, it is observed that the opening and closing doesn't occur at the same degree of the rotation of the cycle which means the cracking pressure of the valve is affected with change in the spring preload of the valve.

4.4 Simulation and Results

4.4.1 Engine in a stationary state

The experiments were done on the test engine in stationary conditions which means the engine speed was zero rpm. Therefore the pressure inside the pre-chamber remains constant and is measured to be 0.98 bar. The aim was to see the dependence of the gas input pressure on the cumulative volumetric flow rate through the check valve and fuel injection system. The operating gas used for the experiment was Nitrogen (N_2) with a standard density of 1.2504 kg/m^3 at 0^o C and atmospheric pressure.

The input pressure of the gas was varied between 1.5-2.3 bar. Gas flow was measured and controlled by an OMEGA FMA2610A mass flow controller. The measurement of the flow rate was taken upstream of the check valve by the mass flow meter as shown in figure 11. The gas was allowed to flow through the system and after waiting for some time when the steady-state condition was observed, measurements were taken with the help of data acquisition system complied with LABVIEW.

Results from the experiment and GT suite simulation are listed below:

Case no	Input Pressure (bar)	Input Temperature (^oC)	Pre-chamber Pressure (bar)	Vfr(Standard m^3/h) (Experimental)	Vfr(m^3/h) (Gt suite)	Error (%)
1	2.321	22.12	0.98	1	0.9923	0.77
2	2.273	21.3	0.98	0.97	0.9519	1.87
3	2.083	20.5	0.98	0.79	0.7786	1.44
4	1.889	21.8	0.98	0.59	0.5963	-1.07
5	1.827	21.7	0.98	0.51	0.5306	-4.04
6	1.71	21.9	0.98	0.4	0.433	-8.25
7	1.499	21.6	0.98	0.2	0.2059	-2.95

Table 4 Experimental and simulated data for the steady-state condition

As seen from the table the experimental data doesn't give us any evidence about the check valve performance or any of its parameters. Hence we have to rely on the simulated results for the same. The idea behind the simulation was to apply the above boundary condition in the fuel injection system model and run the simulation with different mechanical parameters and compare the results for the flow rate with experimental results. It was observed that the mechanical parameter of the valve-like spring stiffness and preloading have a direct impact on the flow rate which is discussed in the previous section.

Therefore to calibrate the model and find the mechanical parameters, the methodology mentioned in the section [4.2] is applied and results were obtained.

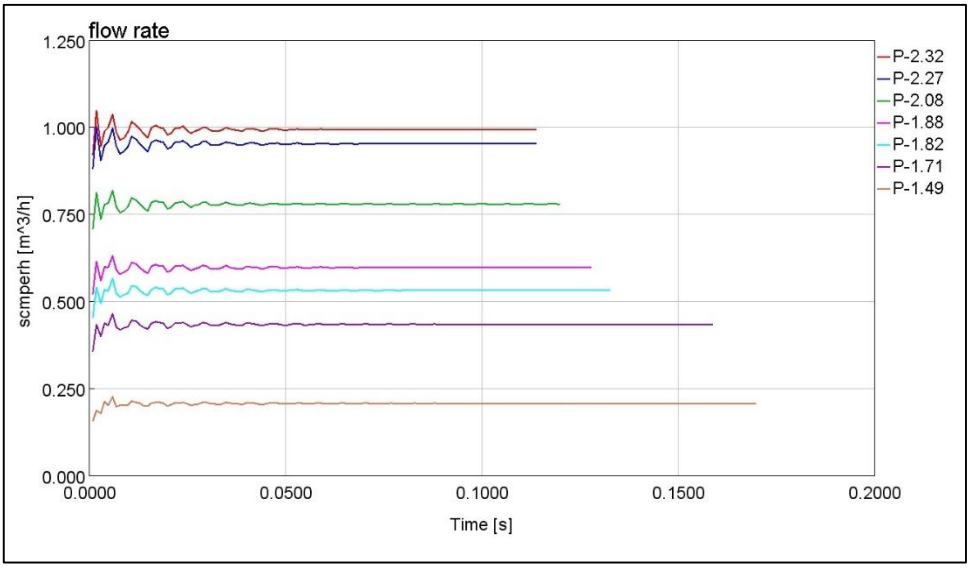

Figure 16 Volumetric flow rate(m^3/hr)- steady-state condition

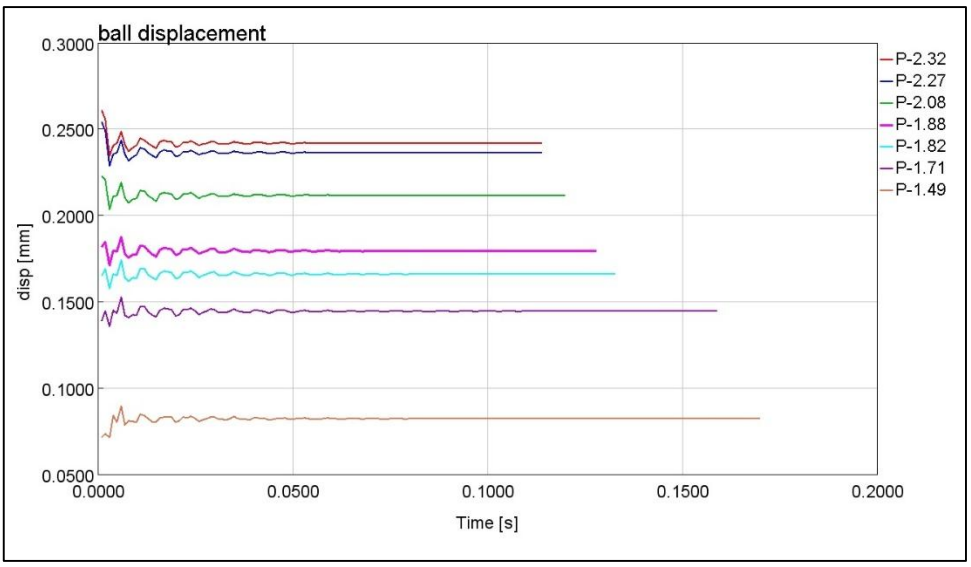

Figure 17 Ball displacement(mm) - steady-state condition

FIGURE 16 and 17 show the simulation results from the GT POWER model for the volumetric flow rate and displacement of the ball. It can be noticed that for different input pressure the convergence time is different.

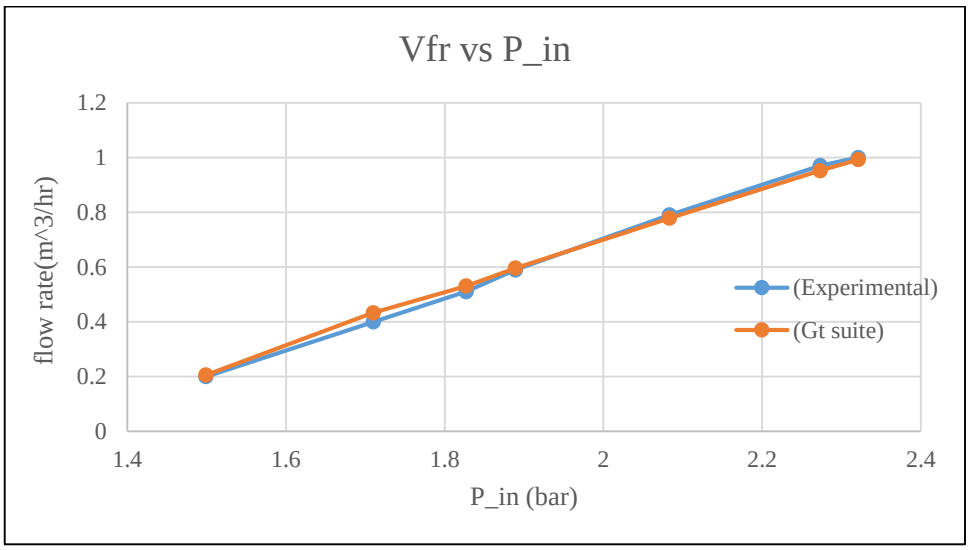

Figure 18 Plot of Comparison of Volumetric flow rate(m^3/hr) versus input pressure(bar) between experimental data and simulation results

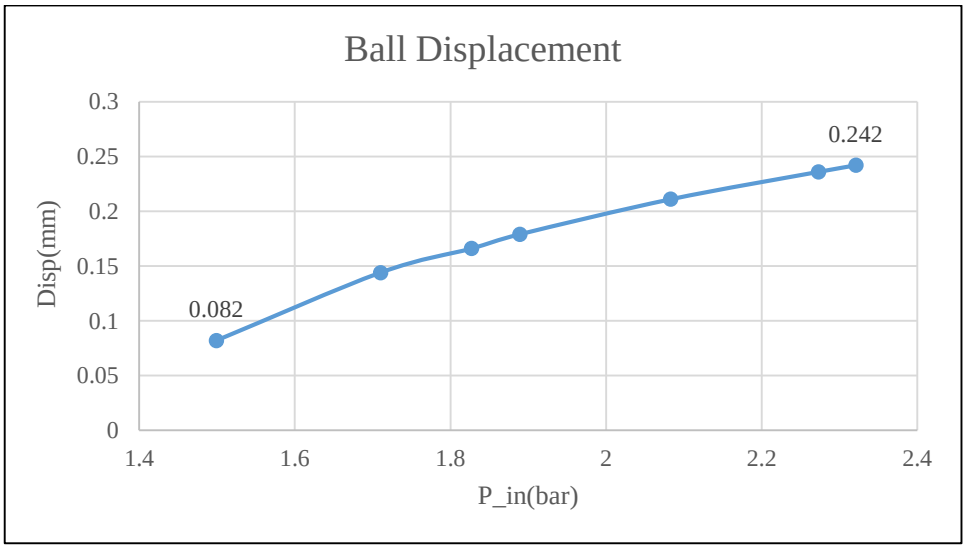

Figure 19 Ball displacement(mm) versus Input pressure(bar)

` FIGURE 18 shows the plot for the volumetric flow rate in m^3/hr and the comparison of the simulated data from GT power with experimental values. The simulation result shows a maximum error of -8% compared to the experimental result at the lower input pressure of the gas. For the gas input pressure above 2 bar, the error is within 2% of the experimental values. Mechanical parameters were iterated for all the points in the curve to find the best fit for the results. One interesting thing to notice from figure 19 is that max displacement of the ball at an input pressure of 2.3 bar is

0.242 mm with a min displacement of 0.082 mm at 1.49 bar pressure. The maximum possible ball movement based on the design of the valve is 1.022 mm. It was noticed during the simulation that spring stiffness and preloading of the spring influenced the ball lift so as affecting the flow rate.

TABLE 5 shows the values of spring stiffness and preloading obtained at the end of the simulation.

Parameter	Value	Unit
Stiffness	0.44	N/mm
Preload	**0.082**	**N**
	31.87	**kPa**

Table 5 Predicted Mechanical Parameters- steady-state case

Preload of the spring corresponds to the cracking pressure of the valve which is in range of the cracking pressure provided by the manufacturer and can be seen in the Attachment B.

4.4.2 Unsteady-state Engine conditions

In the engine laboratory, the tests were conducted on the engine in a running state with different operating conditions. This section will help us understand the behavior of the ball check valve during the engine operation. The check valve opening and closing can be monitored for engine cycles with the help of results from the GT-POWER model. The same methodology has been used here as the previous case. The Volumetric flow rate was tuned with iterating the mechanical parameters of the ball valve. Natural gas was used for the experiments which contain 98.4 % of methane. The standard density of the natural gas is 0.7175 kg/m^3 at 0^{o}C and atmospheric pressure. The stoichiometric air-fuel ratio of natural gas is 17.12.

The model was set with the same boundary conditions as that of the experimental engine. The measured pressure in the pressure damping vessel(pNG5) and the corresponding temperature was the input conditions given to the model. The output boundary conditions were the instantaneous pressure profile recorded by the AVL GU13Z-24 miniature pressure transducer installed in the pre-chamber and the corresponding instantaneous temperature profile. The model was simulated at the speed similar to the engine operating speed.

i. Case 1: Constant input fuel pressure and λ-sweep

The test was conducted on the experimental engine at the speed of 1800 rpm. The pre-chamber was fueled with constant fuel input pressure thus the flow rate passing through the ball valve was observed to remain constant. The mixture is made leaner by controlling the air flowing in the cylinder with the help of a conventional throttle valve. A decrease in the Brake mean effective pressure (BMEP) of the engine is observed from the measurements as the mixture becomes leaner. The engine is able to operate with a range of mixture composition with different lambda values. The goal here is to study the behavior of the fuel injection system to the pre-chamber especially the check valve with varying engine performance with changing operating conditions and also to estimate the mechanical parameters of the check valve.

TABLE 6 shows the data measured during the test and the simulation results.

Case no	Input Pressure	Vfr(m^3/h)	Lambda	Vfr(m^3/h)	Error
	(bar)	(Experimental)		(GT Suite)	
1	1.46	0.15	0.985	0.151	-0.67
2	1.47	0.148	1.048	0.147	0.68
3	1.46	0.15	1.226	0.153	-2.0
4	1.45	0.151	1.651	0.145	3.97
5	1.44	0.15	1.898	0.142	5.33

Table 6 Experimental and simulated data - Unsteady State condition- CASE 1

The model was simulated in order to tune the volumetric flow rate and mechanical parameters were estimated for the case. The plots of instantaneous mass flow rate and displacement were obtained from the simulation which helps us understand the behavior of the check valve.

Figure 20 shows the plots of the volumetric flow rate with respect to engine lambda from the experiment and comparison with the simulation results. A max difference of 5% was observed between the simulated and experimental results. The mechanical parameters were iterated for the whole set of points from the curve to find the best results. The estimated mechanical parameters are seen in Table 7. It is observed that the preload has changed from the previous results.

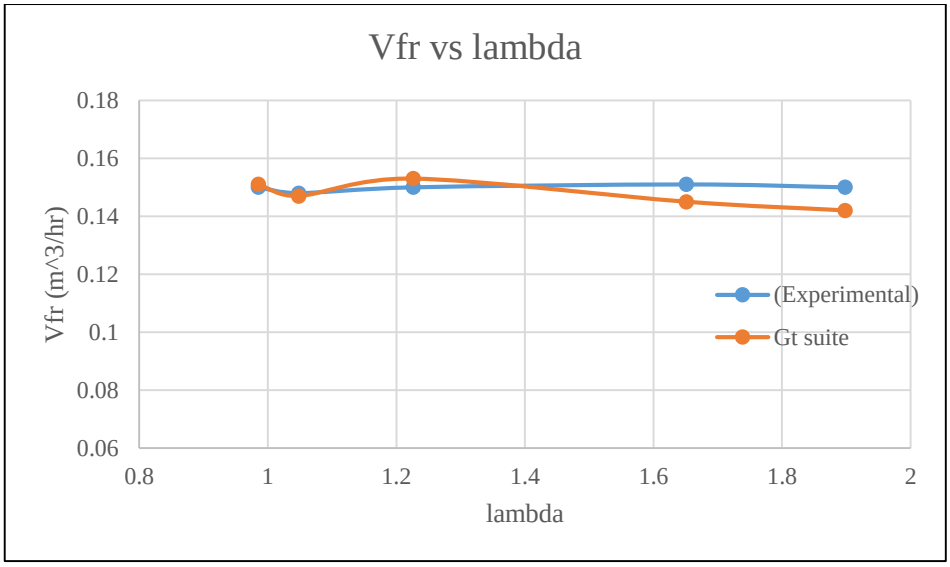

Figure 20 Plot of Comparison of Volumetric flow rate(m^3/hr) versus lambda between experimental data and simulation results - CASE 1

Parameter	Value	Unit
Stiffness	0.44	N/mm
Preload	**0.04**	**N**
	15.55	**kPa**

Table 7 Predicted Mechanical Parameters- unsteady state condition- CASE 1

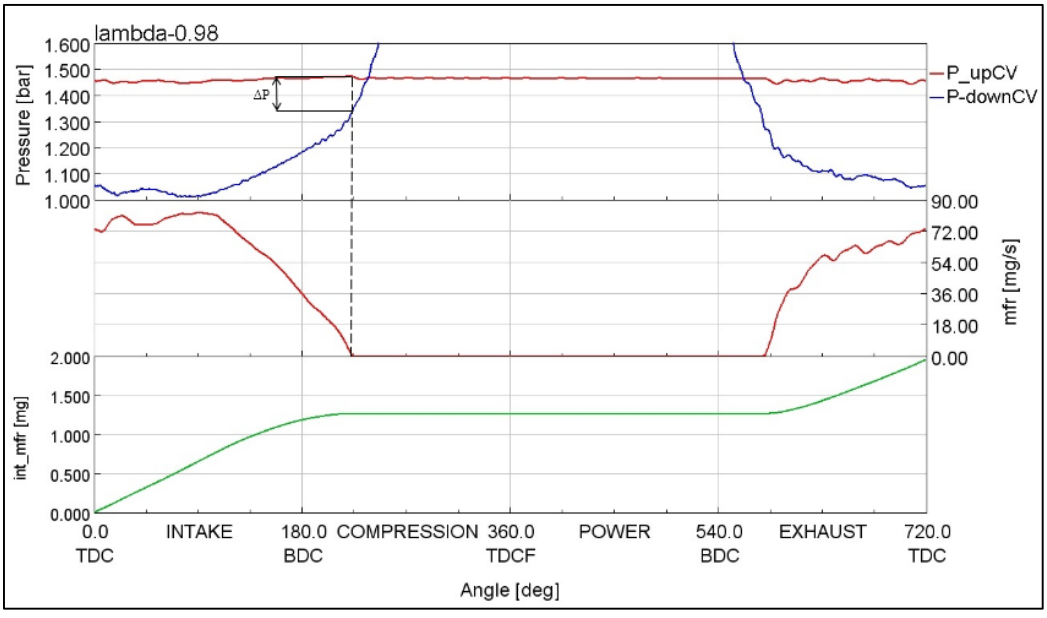

Figure 21 Results from the simulation, Pressure profile upstream and downstream of the valve(upper plot), instantaneous mass flow profile(middle plot), Integrated mass flow rate(lower plot)- lambda 0.98- CASE 1

The plot in figure 21 shows instantaneous pressure profile upstream and downstream of the check valve, the instantaneous mass flow profile and integrated mass flow rate delivered to the pre-chamber obtained from the simulation results for a single-engine cycle for 1st case at lambda=0.98.

Fuel delivered to the pre-chamber is given by the pressure difference between upstream and downstream of the check valve. As the pressure in the pre-chamber(P-down) falls below the value of the pressure loss at the check valve(ΔP=15.5 kPa) the fuel starts flowing into the pre-chamber. The middle plot shows the mass flow profile predicted by the GT-Power simulation. It is seen the 68% of the mass flow is delivered during the intake stroke and the remaining is delivered during the exhaust stroke of the cycle.

No conclusions can be drawn as of now for the fuel which is delivered to the pre-chamber during the exhaust stroke. Only CFD studies will help us understand it. The fuel leak doesn't take part during the main combustion event, therefore it might affect the unburnt hydrocarbons or might be lost during the exhaust stroke only future results will be able to conclude it.

Similar trends were observed for the other cases too. The Plot in figure 18 shows the comparison of the results at lambda 0.98 and 1.98. It can be seen that the fuel leak is present during the exhaust stroke in both cases because the opening of the valve is driven only by the differential pressure across the valve. The maximum ball displacement of 0.134 mm is predicted by the GT-power.

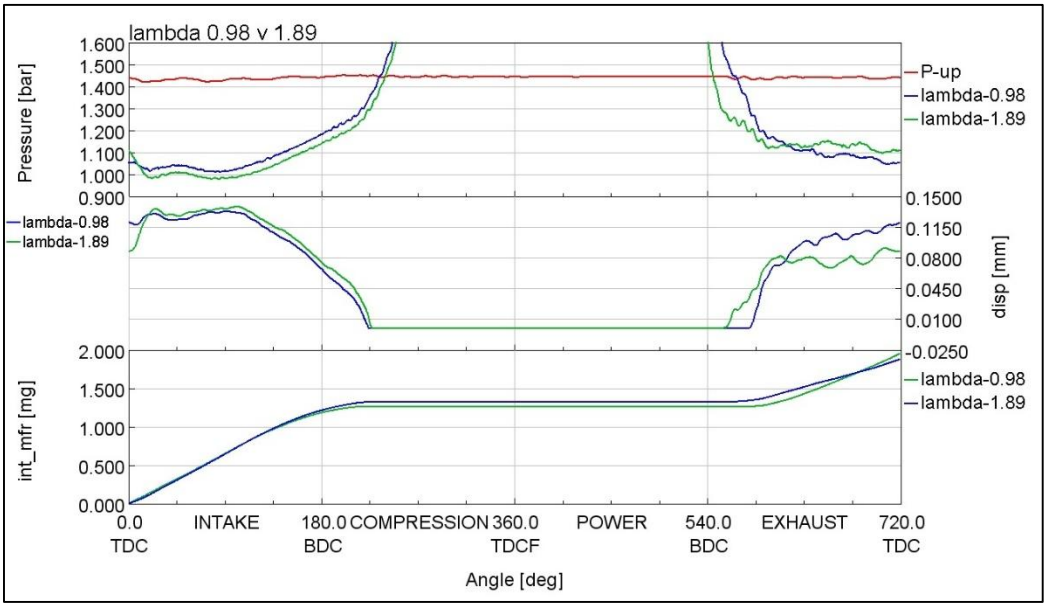

Figure 22 Pressure profile upstream and downstream valve(upper plot), instantaneous mass flow profile(middle plot), integrated mass flow rate (lower plot) lambda 0.98 versus lambda 1.98- CASE 1

ii. CASE- 2: Increasing Fuel input pressure and constant lambda

The test was done on the experimental engine to see the performance in the lean combustion of the air-fuel mixture with the lambda of 1.6 and increasing the fuel delivery pressure to the pre-chamber. The fuel-air mixture supplied to the engine cylinder was varied to maintain constant lambda operations. The test was conducted at an engine speed of 1800 rpm with natural gas as the primary fuel. The volume flow rate passing through the check valve was measured using the OMEGA mass flow meter. The obtained experimental data and simulation results are shown in TABLE 8 below

Case no	Input Pressure	Vfr(m^3/h)	lambda	Vfr(m^3/h)	Error
	(bar)	experimental		(GT Suite)	
1	1.226	0.098	1.687	0.098	0
2	1.302	0.155	1.668	0.157	-1.29
3	1.374	0.207	1.627	0.205	0.98

Table 8 Experimental and simulated data - Unsteady-State condition- CASE 2

The GT POWER model was simulated with boundary conditions similar to the experimental engine and was tuned for the volumetric flow rate by iterating the mechanical parameters of the check valve. Figure 23 shows the plot of the flow rate passing through the check valve measured experimentally and comparison of its simulated data. The graph is plotted with respect to the fuel input pressure to the check valve. An error of -1.29% is observed between the results for input pressure 1.302 bar. For the other two data points, the error is less than 1%. TABLE 9 shows the predicted mechanical parameters of the valve.

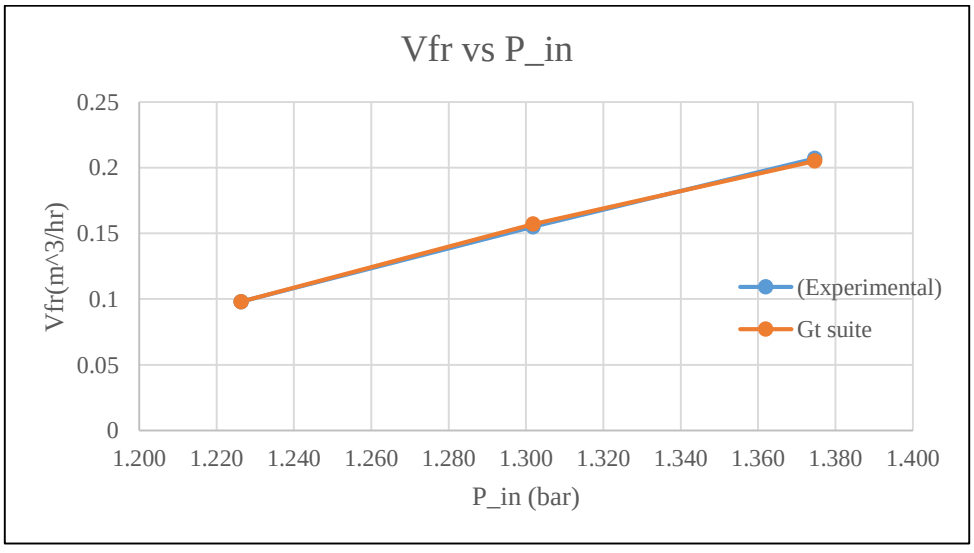

Figure 23 Plot of Volumetric flow rate(m^3/hr) versus input pressure(bar) comparison between experimental and simulation data - CASE 2

Parameter	Value	Unit
Stiffness	0.42	N/mm
Preload	**0.014**	**N**
	5.44	**kPa**

Table 9 Predicted Mechanical Parameters- unsteady state condition- CASE 2

The upper plot in figure 24 shows the instantaneous mass flow profile of fuel delivered to the pre-chamber and passing through the ball check valve for different fuel input pressure. The middle plot indicates the integrated mass flow to the pre-chamber increases as the input pressure increases. The ball displacement is the function of the fuel input pressure. It is higher at high input pressure and can be observed in the lower plot.

The fuel leak during the exhaust stroke is seen in all the cases irrespective of the fuel input pressure to the valve. The fuel losses are maximum at the higher input pressure with max ball displacement expected to be 0.18 mm. For the lower input pressure, the max ball displacement is 0.12 mm during the intake stroke and 0.06 mm during exhaust with a fuel leak of 28%.

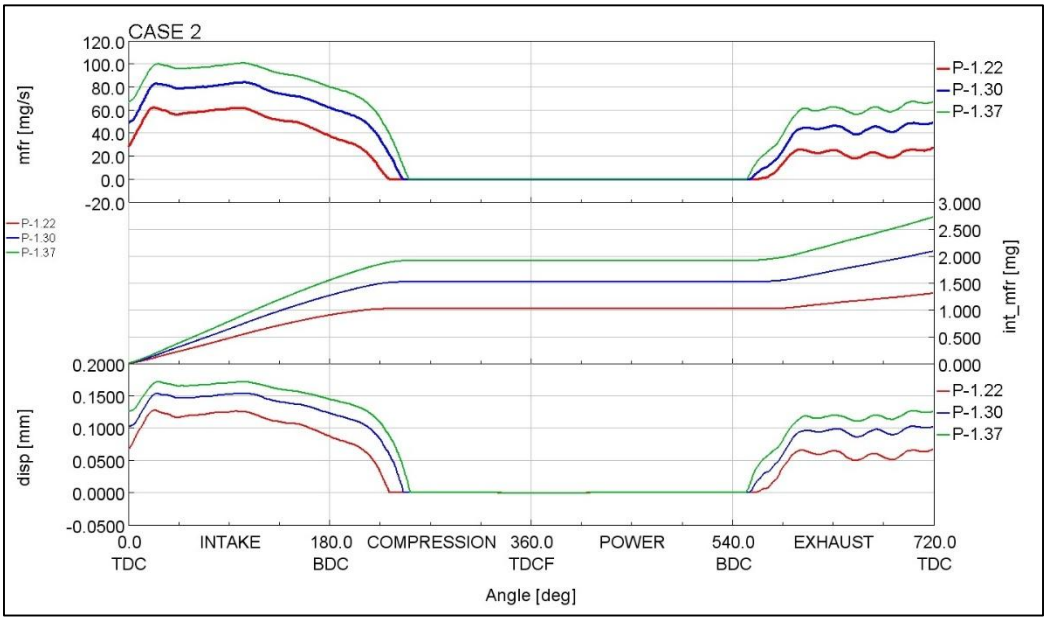

Figure 24 Instantaneous mass flow profile for one cycle(upper plot), Integrated mass flow rate (middle plot), Ball displacement in check valve(lower plot)-CASE 2

iii. CASE-3: Speed Dependance and constant fuel input pressure

The test was conducted on the experimental engine to see the performance at different operating speeds. The pressure of the fuel injected to the pre-chamber was kept constant at 1.2 bar. The main combustion chamber operates in the lean fuel-air mixture with lambda varying between 1.5-1.7. The engine was operated with a speed range of 1200-1800 rpm and readings were taken. TABLE 10 shows the experimental data and simulation results.

Case no	Input Pressure	Engine Speed	Vfr(m^3/h)	lambda	Vfr(m^3/h)	Error
	(bar)	(rpm)	(Experimental)		(GT suite)	
1	1.22	1200	0.105	1.789	0.103	1.9
2	1.22	1400	0.103	1.649	0.104	-0.97
3	1.23	1600	0.1	1.562	0.099	1.98
4	1.22	1800	0.097	1.528	0.100	-3.09

Table 10 Experimental and simulated data - Unsteady State condition- CASE 3

The fuel injection system model was simulated with boundary conditions identical to the experimental setup and tuned for the volumetric flow rate with the same methodology as mentioned in section [4.2]. The mechanical parameters were obtained from the simulation results. Figure 25 shows the results obtained for the flow rate from simulation and the comparison of it with the experimental data. The curves of the results are almost evenly matched, but an error of 3% is seen at the 1800 rpm speed.

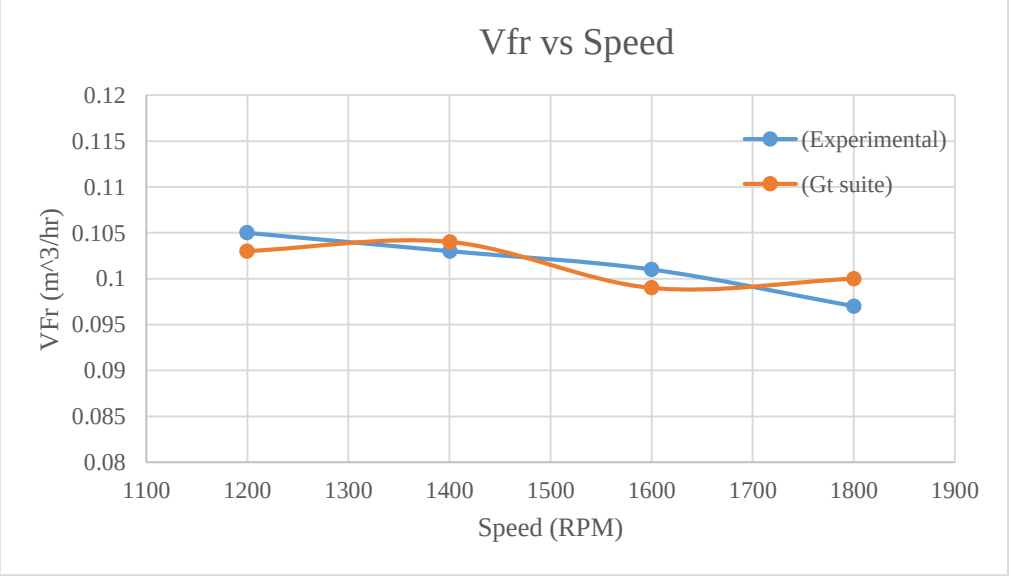

Figure 25 Plot of volumetric flow rate(m^3/hr) versus Engine speed(RPM) comparison between experimental and simulation results- CASE 3

TABLE 11 shows the obtained values of the mechanical parameters after tuning the model. A drop in the values of the mechanical parameters was observed here as compared to the previous simulation.

Parameter	Value	Unit
Stiffness	0.4	N/mm
Preload	**0.0095**	**N**
	3.69	**kPa**

Table 11 Predicted Mechanical Parameters- unsteady state condition- CASE 3

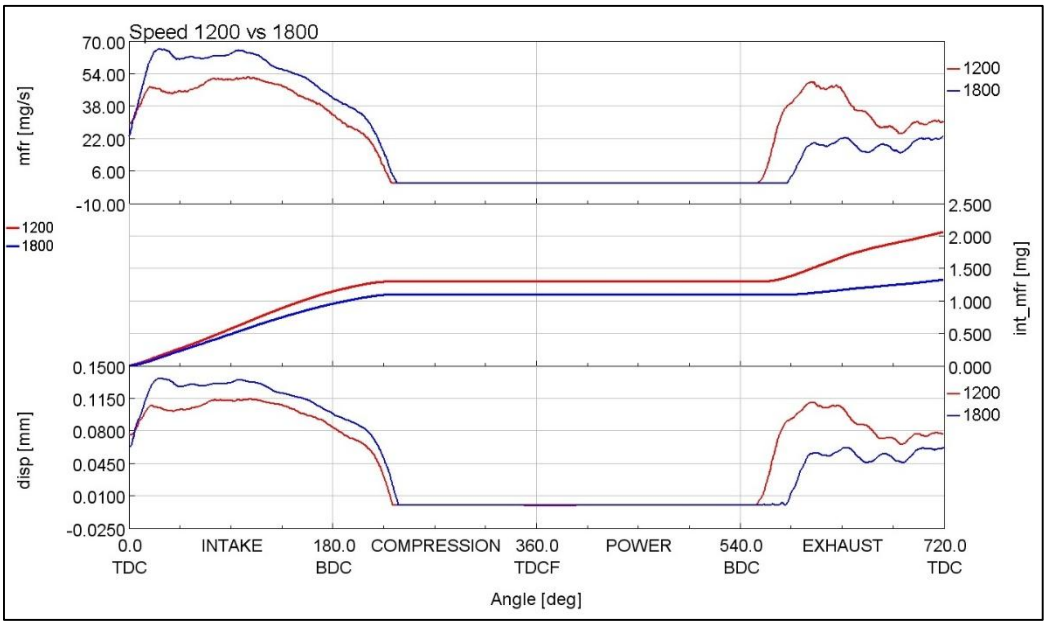

Figure 26 Instantaneous mass flow profile for one cycle(upper plot), Standard volumetric flow rate (middle plot), Ball displacement in check valve(lower plot)-CASE 3

The upper plot in figure 26 shows the comparison of the instantaneous mass flow of a single cycle for an engine operating speed of 1200 and 1800 rpm. The fuel delivery pressure to the pre-chamber is constant at 1.22 bar. It is observed from the simulation results, the fuel leak during the exhaust stroke is minimum at the engine speed of 1800 rpm. The fuel leak at 1800 rpm engine speed is about 32%. At 1200 rpm comparatively higher amount of fuel is delivered to the pre-chamber during the exhaust stroke.

For the speed dependence, the fuel leak to the pre-chamber is predicted since the only driving parameters for the opening of the ball valve is its cracking pressure.

iv. CASE-4: Increasing fuel pressure and Engine mode – C [13]

The test was conducted on the experimental engine with operation mode – C which is Partly motored mode means the fuel was delivered only to pre-chamber and ignition takes place. This mode evaluates the combustion efficiency of the combustion process in the pre-chamber and to quantify the ignition energy from the pre-chamber combustion. The main chamber was filled with air instead of a lean fuel-air mixture. The engine operational speed was 1800 rpm. The data obtained from the experiments and simulation results are seen in TABLE 12.

Case no	Input Pressure	Engine Speed	Vfr(m^3/h)	Lambda (in the exhaust)	Vfr(m^3/h)	Error
	(bar)	(rpm)	(Experimental)		(GT suite)	
1	1.16	1800	0.102	36.826	0.098	3.92
2	1.30	1800	0.196	20.233	0.198	-1.02
3	1.45	1800	0.304	13.145	0.325	-6.9

Table 12 Experimental and simulated data - Unsteady-State condition- CASE 4

It should be noted that this operation mode (Mode C) is not typical for the normal engine operations. It is used to study the pre-chamber functionality and mainly used for the CFD simulations. The aim here to see the performance of the check valve in such operating conditions. The instantaneous pressure profile in the pre-chamber measured by the pressure transducer for such operating condition can be seen in figure 27.

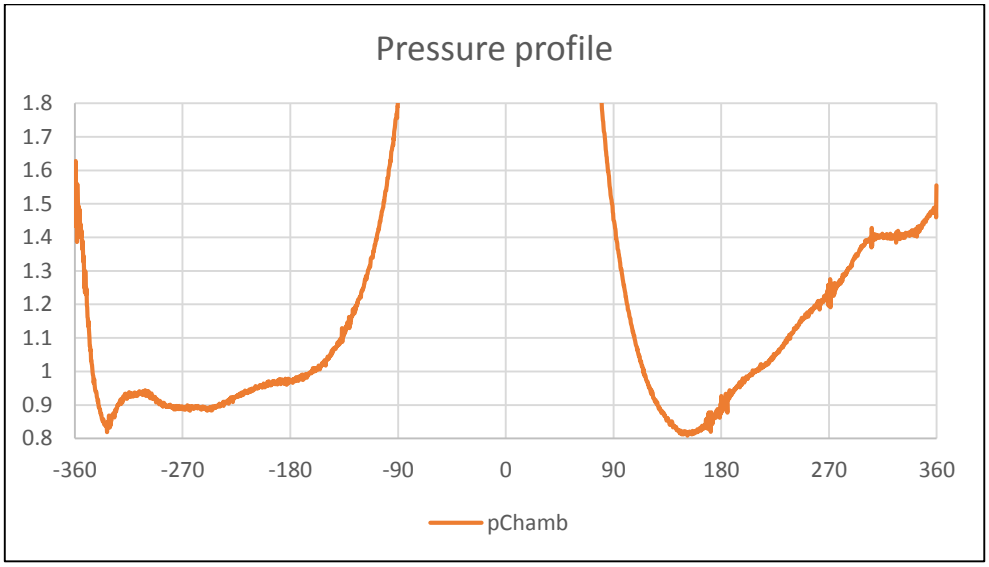

Figure 27 Pre-chamber pressure plot

The boundary condition for the GT power was set similar to the experimental engine except for the fact that the instantaneous pressure profile of the main combustion chamber was used as an output boundary condition. Adrift was observed in the pressure profile of the pre-chamber. A detailed explanation is presented in section [4.4.3]. The results show the dependence of the flow rate with respect to the fuel injection pressure to the pre-chamber except that the main chamber is filled with air only.

The model was calibrated for the volumetric flow rate and the mechanical parameters were predicted for this case. Figure 28 shows the comparison of the experimental results compared to the simulation results. The data point for input pressure less than 1.3 bar is evenly matched whereas an error of -6% is seen at high input pressure. Mechanical parameters were calculated to find the best fit for the results. TABLE 13 shows the predicted mechanical parameters for this case.

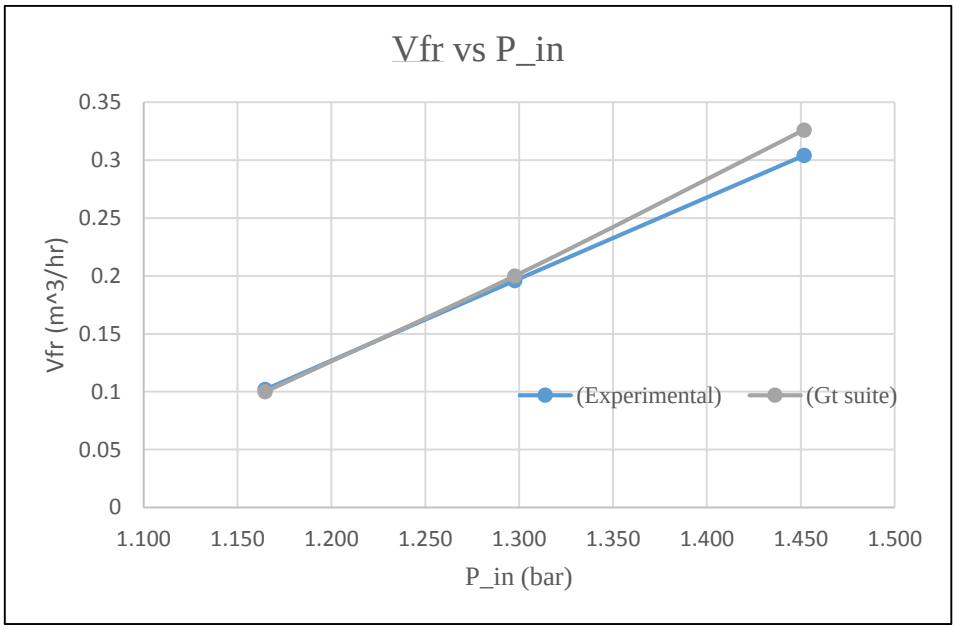

Figure 28 Plot of Volumetric flow rate(m^3/hr) versus input pressure(bar) comparison between experimental and simulation data - CASE 4

Parameter	Value	Unit
Stiffness	0.4	N/mm
Preload	**0.0015**	**N**
	0.58	**kPa**

Table 13 Predicted Mechanical Parameters- unsteady state condition- CASE 4

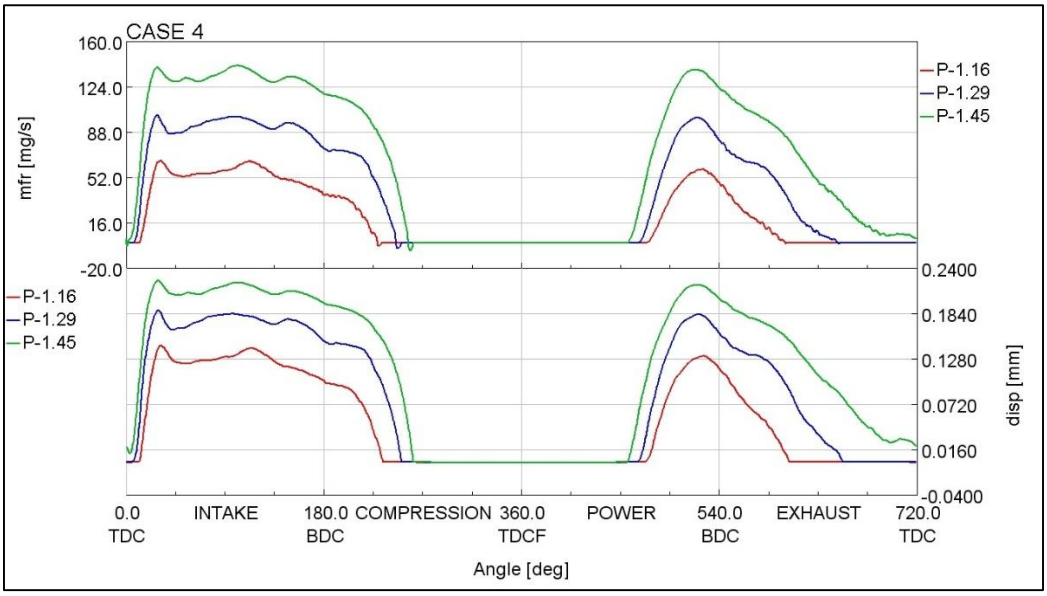

Figure 29 Instantaneous mass flow profile(upper plot), Ball displacement(lower plot) – Pressure 1.16 vs 1.29 vs 1.45

The plot in figure 29 shows the instantaneous mass flow to the pre-chamber and the displacement of the ball for an engine cycle for different fuel input pressure. It is seen the fuel is delivered at the end of the power stroke and early exhaust stroke when the engine is operated in MODE C. That means a huge amount of the fuel is leaked during this period which doesn‘t take part in the main combustion process. Although this operation mode is not typical for the engine, it is evidence that the opening of the ball valve is solely dependent on the differential pressure across the valve. In other words, at constant fuel input pressure, the opening of the valve is driven by the instantaneous pressure downstream of the ball valve which is pre-chamber pressure. Figure 30 shows the pressure profile upstream and downstream of the valve for fuel input pressure- 1.45 bar.

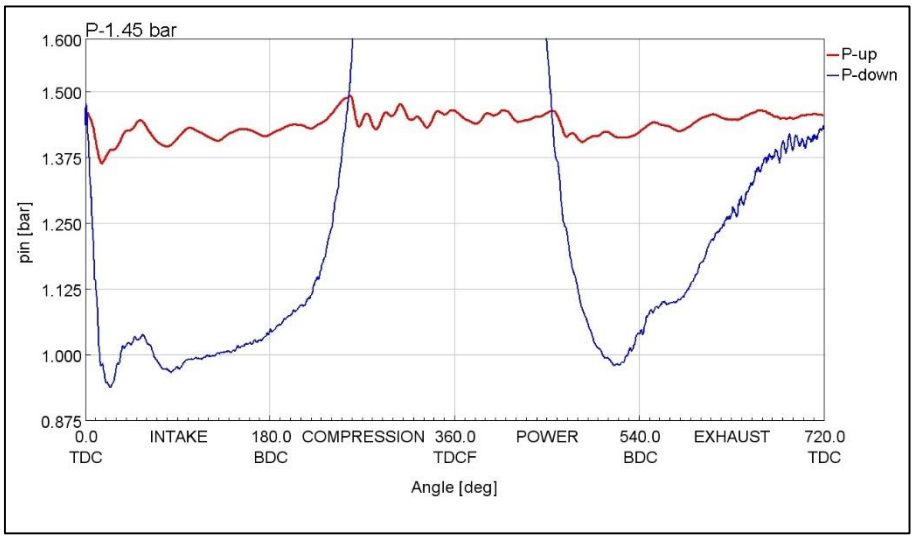

Figure 30 Pressure upstream and downstream on the check valve at Pressure 1.45 bar

4.4.3 Thermal drift in pressure measurement

An uncooled AVLGH15D pressure transducer is installed in the pre-chamber to record the pressure signals. The pressure signals recorded were amplified using the two-channel Kistler charge amplifier. The specifications of the pressure transducer are mentioned in FIGURE 31.

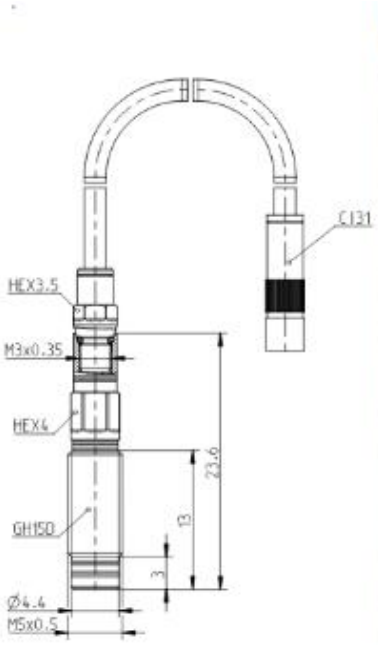

Specifications			
Measuring range		0...250 bar	
Overload		300 bar	
Lifetime	≥	10^8	load cycles
Sensitivity		19 pC/bar	nominal
Linearity	≤ ±	0.3%	FSO
Natural frequency	~	160 kHz	
Acceleration sensitivity	≤	0.0005 bar/g	axial
Shock resistance	≥	2000 g	
Insulation resistance	≥	10^{13} Ω	at 20°C
Capacitance		7.5 pF	
Operating temperature range		-40°C...400°C	
Thermal sensitivity change	≤	1%	20... 400°C
	≤ ±	0.25%	250 ±100°C
Load change drift		1.5 mbar/ms	max. gradient
Cyclic temperature drift [1]	≤ ±	0.5 bar	
Thermo shock error [2]			
Δp	≤ ±	0.3 bar	
Δp_m	≤ ±	1.5%	
Δp_{max}	≤ ±	1%	
Thread diameter		M5x0.5	front sealed
Cable connection		M3x0.35	negative
Weight		2.2 grams	without cable
Mounting torque		1.5 Nm	

Figure 31 Specifications of the AVLGH15D pressure transducer [22]

The pressure transducer is installed in the pre-chamber in the vicinity of the spark plug and the fuel delivery capillary to the pre-chamber since the pre-chamber has very low volume. The operating temperature range as mentioned in the specifications is -40 to 400^{o}C. However, the temperature in the pre-chamber exceeds more than 1400^{o}C during the normal engine operations. The transducer has to records the pressure signal in such a high-temperature environment which is beyond its designed range.

Flame arrestors

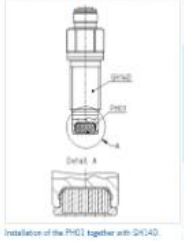

Thermo protection	Art.No.	Recommended for	Cyclic temperature drift without flame arrestor	Typical cyclic temperature drift with flame arrestor
PH01	TIYF0592A.01	GH14D GH14DK GR14D GH15D GH15DK GH13Z	0.5 bar 0.7 bar 0.5 bar 0.5 bar 0.7 bar 0.5 bar	0.3 bar 0.4 bar 0.3 bar 0.3 bar 0.4 bar 0.3 bar
PH03	TIYF0734A.01	GH14D GH14DK GR14D GH15D GH15DK GH13Z	0.5 bar 0.7 bar 0.5 bar 0.5 bar 0.7 bar 0.5 bar	0.3 bar 0.4 bar 0.3 bar 0.3 bar 0.4 bar 0.3 bar
PH04	TIBW7172A.01	GU22C GU22CK GG22C	0.4 bar 0.5 bar 0.4 bar	0.3 bar 0.3 bar 0.3 bar

Figure 32 Flame arrestor details [22]

For the accurate measurement at the high temperature, it is recommended to use the flame arrestors. It is installed at the shown in Figure 32. PH03 flame arrestor when coupled with the GH15D transducer reduces the thermal drift error by 0.2 bar. However, due to extremely less space in the pre-chamber, the pressure transducer is not equipped with flame arrestors.

An AVL GU13Z-24 uncooled miniature pressure transducer is installed in the main combustion chamber to record the pressure signals. It is installed in the cylinder head of the engine. For the MODE – C operation of the engine the fuel is delivered only to the pre-chamber. After the combustion of the fuel-air mixture in the pre-chamber, a flame travels in the form of the jet to the main chamber through the holes which are projected towards the cylinder perimeter. Therefore the pressure transducer is not directly exposed to this flames since it is installed in the cylinder head resulting in a lower temperature in the vicinity thus reducing the thermal drift. Another reason for the high error in pressure signals from the pre-chamber can be the aging of the transducer.

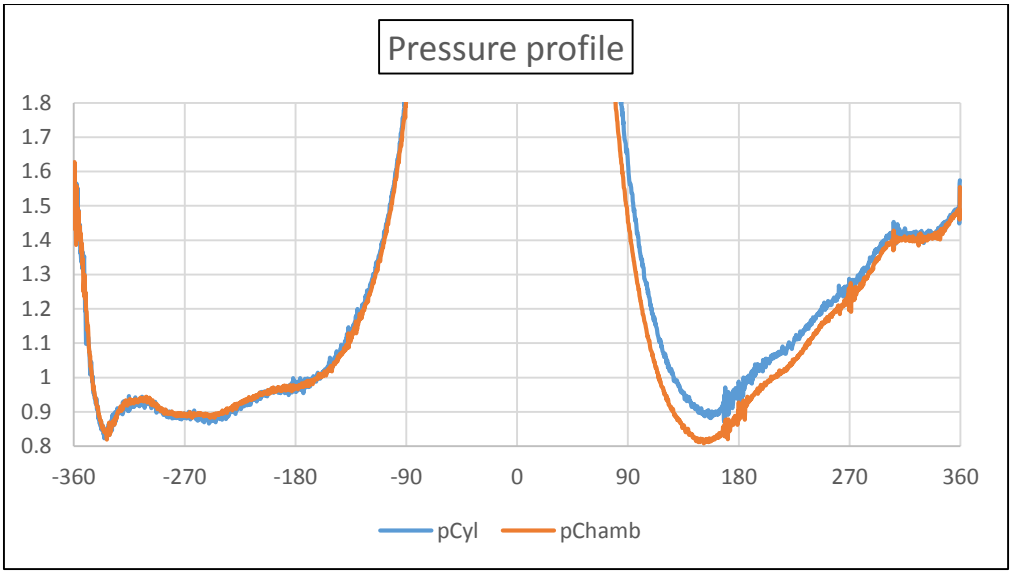

Figure 33 Comparison between Cylinder pressure and pre-chamber pressure profile

Figure 33 the plot of the instantaneous pressure profile of the pre-chamber and the cylinder. Adrift is seen in the pressure profile of the pre-chamber during the exhaust stroke since the operating temperature is very high during that period.

If the pre-chamber pressure profile is used as the boundary condition for the GT power model to simulate the results. An error of 15% is noted in the fuel flow rate. To compensate this error pressure profile from the main engine cylinder (P-cyl) was used as the boundary conditions for the model. Figure 34 shows the instantaneous mass flow profile of the fuel delivered to the pre-chamber, the difference in the fuel flow to the pre-chamber with use of P-chamber profile versus P-cyl profile can be noticed. The

integrated mass flow is also higher and can be seen in figure 35. Since the principle of the opening of the valve is dependent on the differential pressure across the valve.

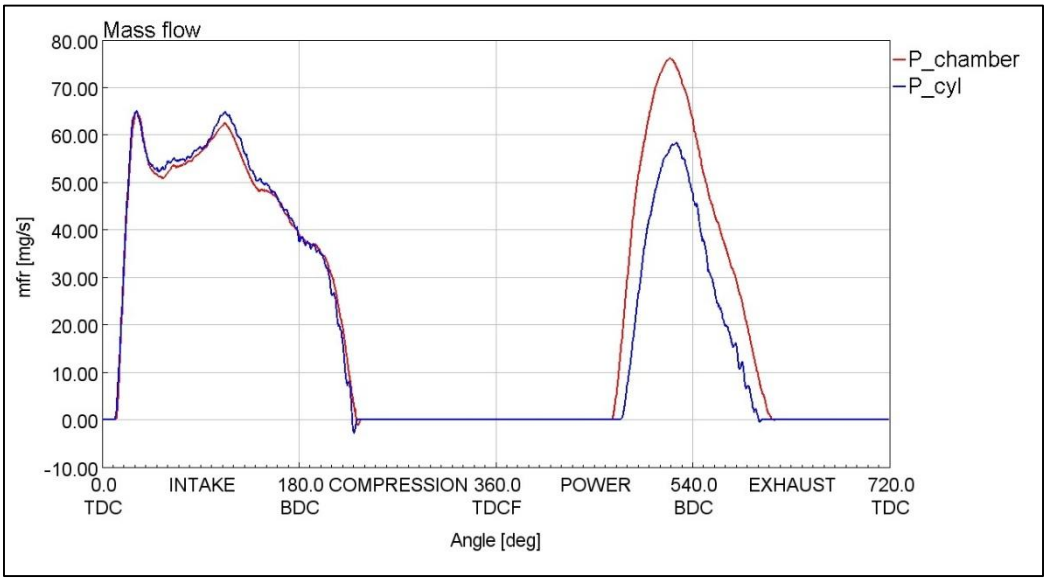

Figure 34 Instantaneous mass flow profile (mg/sec)

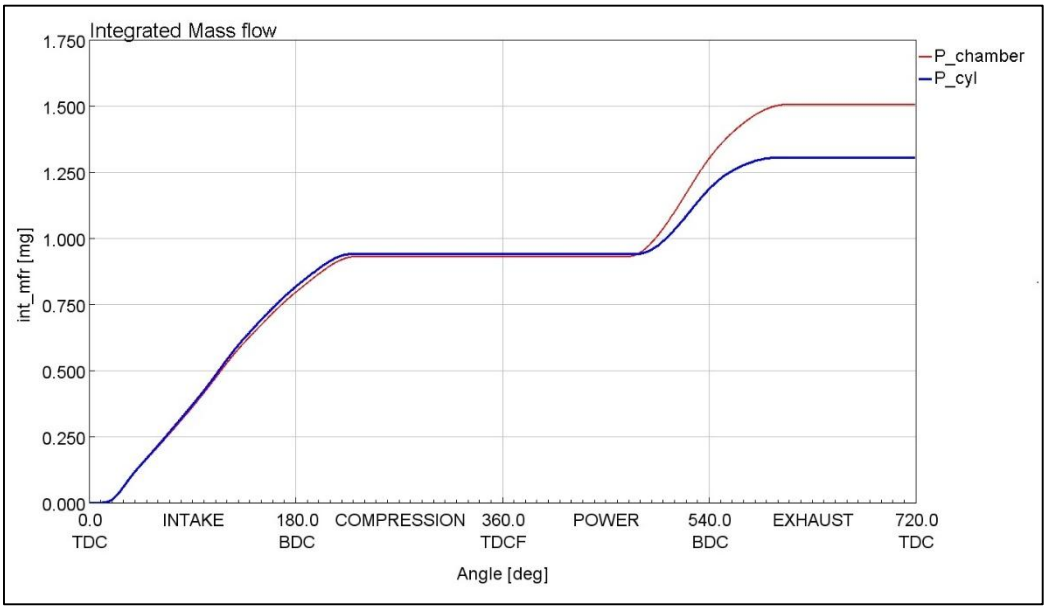

Figure 35 Integrated mass flow rate(mg)

4.5 Summary and comparison of the results

As mentioned earlier due to insufficient data of the check valve, the mechanical parameters of the valve-like spring stiffness and preload were unknown. The simulation was carried out on the GT power model for various operating conditions and are discussed in section [4.4]. The boundary conditions of the model were kept identical to the engine operating conditions, the model was tuned for the fuel flow rate with iterating the mechanical parameters as it directly affects the flow rate.

This section summerise the mechanical parameters predicted at the end of the simulation for each case and gives us an idea about its variation. TABLE 14 shows the values of the mechanical parameters predicted by the GT suite model for different cases.

		Case	Speed	Spring Stiffness	Preload
			(rpm)	(N/mm)	(kPa)
Steady State		Increasing fuel pressure		0.44	31.87
Unsteady State	Date set -1	Lambda sweep & Constant fuel pressure	1800	0.44	15.55
	Date set -2	Increasing fuel pressure & Constant lambda	1800	0.42	5.44
	Date set -3	Speed Dependance& Constant Fuel pressure	1200-1800	0.4	3.69
	Date set -4	Engine mode C & Increasing fuel pressure	1800	0.4	0.58

Table 14 Summary and comparison of predicted mechanical parameters

The tests on the experimental engine were done over a while. The initial test performed on the engine was the steady-state test in which the engine was not in a running condition. A new check valve was installed in the setup and the test was done with varying fuel input pressure feeding the pre-chamber. The GT power model was simulated with identical boundary conditions as that of the experimental engine and calibrated for the flow rate measured experimentally with the help of OMEGA mass

flow meter. The mechanical parameters were iterated to find the best fit to achieve the results within the desired tolerance.

From the GT power results, a spring stiffness of 0.44 N/mm and spring preload of 31.87 kPa was predicted. The accuracy of these results is difficult to predict as no evidence or data confirming it. With the help of these parameters, the fuel injection model was simulated and the output flow rate passing through the ball valve is in the desired tolerance as that of the experimental data and can be seen in figure 18. Also, the predicted initial spring preload of 31.87 kPa is in the range of the preload/cracking pressure given in the manuals provided by the LEE, manufacturers of the check valve. Thus, due to insufficient data, we had to depend on the simulation results for the values of the mechanical parameters and proceed further for the simulation.

The same check valve is used for the further test on the engine over the period and it is observed that there is a significant drop in the spring preload of the check valve from to 31.89 kPa to 0.58 kPa. The reason for this drop cannot be exactly specified. One reason for the variation can be, the spring loses its pretension over the period during the operation and it cannot be restored. The loss in the pretension of the spring affects its stiffness as well but there is a marginal change as compared to its initial value.

Now, we know the mechanical parameters of the valve we can confirm that the fuel injection model can be set up completely when it will be coupled with the single-cylinder research engine model and further studies for larger speed range can be carried out. This mechanical parameter will also help us carry out the model analysis of the check valve to find out the eigenfrequencies of the valve and assess for the resonance conditions.

The results suggest that it thus become necessary to replace the check valve after a specific interval of the operation to ensure the proper functioning of the check valve. The loss in pretension and the spring stiffness will affect the flow rate passing through the valve. A sensitivity analysis of these parameters was initially carried out to see the effect on the flow rate and can be seen in section 4.3.

5. Single Cylinder Research Engine

A single-cylinder 4-stroke engine with a higher working speed range is designed by the Czech Technical University, Prague and manufactured by SKODA AUTO. The test on this experimental engine will be done at VTP Roztoky.

The engine has a bore of 74.5 mm and a stroke of 85.9 mm with a compression ratio of 10.8. The engine will be tested with natural gas as the primary fuel. The engine has two injection systems. The fuel is sprayed in the intake port with help of a fuel injector and the engine has its own scavenged pre-chamber design with a separate fuel injection system to the pre-chamber. A LEE manufactured 558 series forward flow check valve will be used in the injection system of the pre-chamber. The check valve has the ball diameter of 2.1 mm and the seat diameter of the 1.8 mm with a max displacement of the ball is restricted by design to 1.022 mm. The further details of the check valve are attached in Attachment B. Since this will be a completely new set up a new check valve will be installed and from the previous studies, the mechanical parameters of the check valve were predicted and are listed in TABLE 15.

Parameters	Value	Units
Spring Stiffness	0.44	N/mm
Preload	31.79	kPa

Table 15 Mechanical parameters of the check valve - LEE 588 series

5.1 Pre-chamber design for high-speed research engine

The cylinder head of the engine is modified for installing the scavenged pre-chamber. A fictitious pre-chamber is designed for the study purpose, modifications will be done to this pre-chamber later as the study progresses. Figure 36 shows the schematic of the current fictitious pre-chamber design.

The volume of the pre-chamber is 515 mm^3 with a diameter of 6 mm. The pre-chamber has its fueling system as seen in the figure. The gaseous fuel will be injected to the pre-chamber through the ball check valve manufactured by the LEE company. The laboratory is equipped with a compressed natural gas (CNG) line with gas pressure up to 200 bar. A pressure regulator will be used to regulate the pressure to approximately 3 bar. Omega mass flow meter OMEGA FMA2610A will control and measure the fuel flow rate.

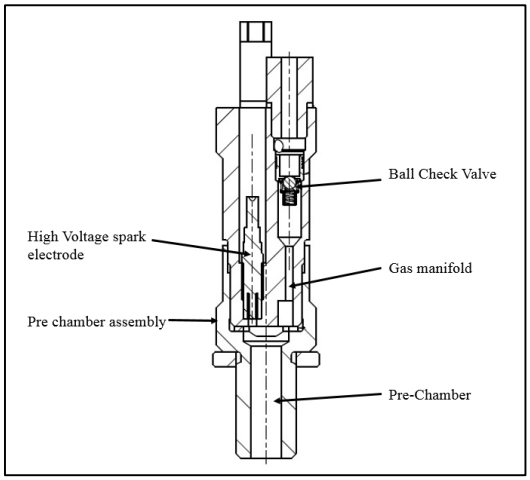

Figure 36 Pre-chamber for High-speed engine

A high voltage spark electrode is also installed to ignite the fuel-air mixture. An uncooled pressure transducer will be installed to records the pressure signal. The installation of the miniature transducer will allow a crank angle resolved pressure measurement in the pre-chamber.

5.2 GT-Power part

A single-cylinder engine model suitable for working at the larger speed range was developed by the predecessors. The combustion model was defined to the main cylinder of the engine. The boundary conditions, run setup and dimensions were set up by the predecessor. The model was not equipped with the pre-chamber initially. This section contains the following part

1) Integrating the new pre-chamber design into the model and modeling the fuel injection system to the pre-chamber with the help of provided geometric data.
2) Setting up the check valve and other required boundary conditions for the fuel injection system.
3) Simulating the model at full load condition of the engine with speed range up to 6500 rpm
4) Monitoring the fuel flow through the check valve for the speed range and studying its behavior.

The results from the simulation will help understand the behavior of the fuel injection system to the pre-chamber at higher engine operating speed, especially the check valve since it is very sensitive and operates automatically without external control. The principle of the operation of the check valve depends on the pressure upstream and downstream of the valve. The basic requirement of the fuel injection

system is, it should deliver the fuel during the intake stroke. Any fuel injected during the exhaust stroke will not take part in the main combustion event and will be accounted as the fuel loss, therefore it should be avoided.

5.3 Full load condition simulation and results

The boundary condition for the single-cylinder engine model was set up by the predecessor, no changes were made to it. The fuel injection system to the pre-chamber was integrated into the single-cylinder engine model and the boundary conditions were set up according to the strategy to be applied while testing the experimental research engine.

The model was simulated at the full load condition of the engine which means fully open throttle with speed range up to 6500 rpm. A constant fuel flow rate of 0.1 m^3/hr controlled by the OMEGA mass flow meter was supplied to the injection system of the pre-chamber at the pressure of 1.59 bar. The fuel-injected in the intake port was varied to have a stoichiometric air-fuel ratio at the start of the combustion to ensure complete burning of the fuel. A control system was developed which controls the fuel sprayed in the intake port. The check valve was set up with the mechanical parameters predicted from the previous studies. The final GT-power model can be in the attachment E.

Following are the results obtained from the simulation:

Figure 37 shows the brake mean effective (BMEP) plot at full load operation of the engine. BMEP is derived from the brake torque which is dependent on the combustion process. Since it is a naturally aspirated engine, the air flowing in the cylinder solely depends on the atmospheric pressure and cylinder pressure. The variation in the BMEP is due to the mass flow of air sucked in the cylinder during the operations. Figure 38 and figure 39 show the brake specific fuel consumption and fuel flow through the pre-chamber and injected by the fuel injector. At 6500 engine rpm, about 98 % of the total fuel during the combustion event in the engine is supplied by the fuel injector. Whereas 93% of the fuel is supplied by the injector at 1500 engine rpm. As the speed reduces the fuel passing through the check valve increases.

Speed(RPM)	6500	6000	5500	5000	4750	4000	3500	3000	2500	2000	1500
Mass thru injector(mg)	23.3	23.7	23.0	21.7	20.2	23.5	21.2	20.9	18.7	21.2	22.6
Mass thru CV (mg)	0.4	0.4	0.4	0.5	0.5	0.6	0.6	0.7	1.0	1.2	1.7

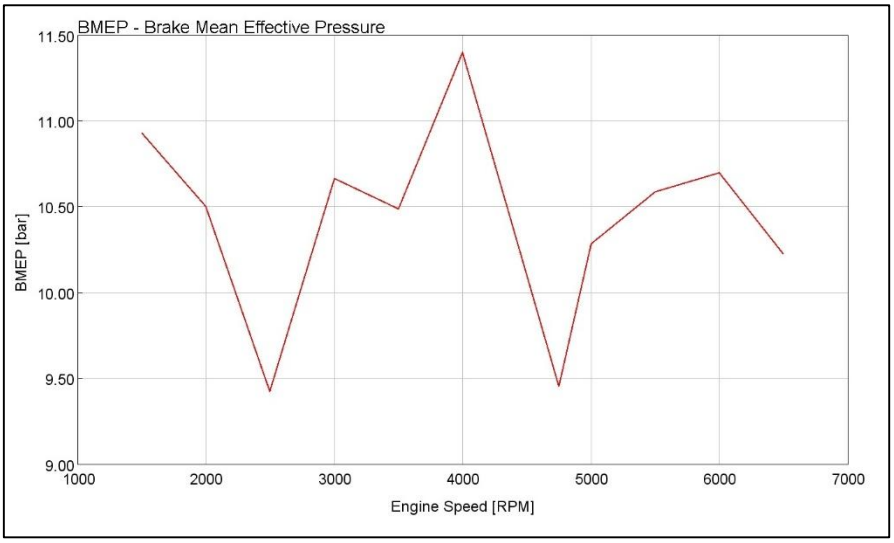

Figure 37 Brake mean effective pressure(bar) vs engine speed (RPM)

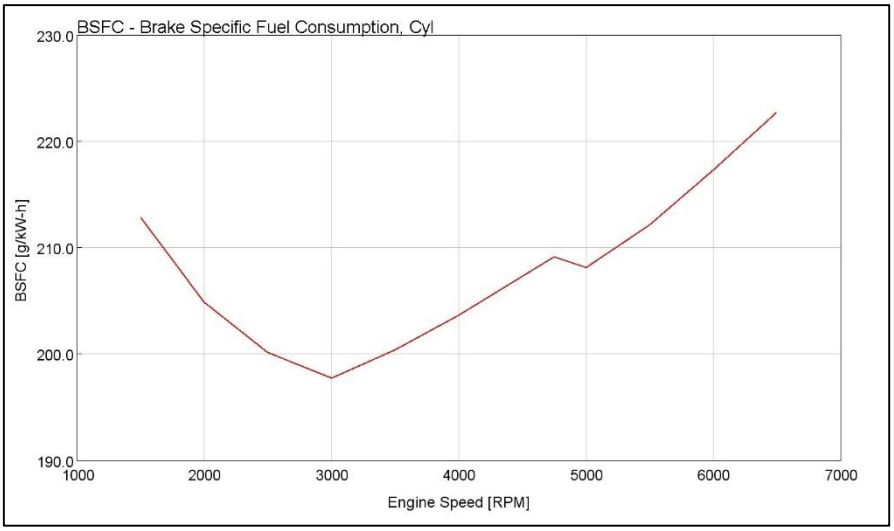

Figure 38 BSFC (g/KW-hr) vs engine speed (RPM)

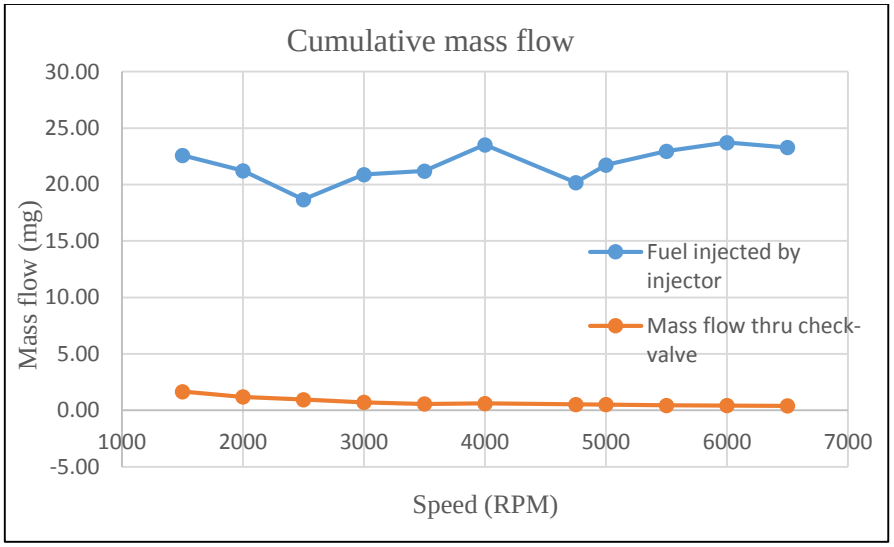

Figure 39 Fuel delivered through pre-chamber and injector

The upper plot in figure 40 represents the pressure profile upstream(input fuel pressure) and downstream(pre-chamber pressure) of the check valve at the engine operating speed of 6500 rpm. As mentioned before the fuel delivery to the pre-chamber is governed by the differential pressure of the valve. It can be seen from the middle plot the fuel is delivered through the check valve only during the intake stroke of the cycle and ends at the early compression stroke. No fuel is delivered during the exhaust stroke of the cycle thus eliminating the fuel losses. The max ball displacement of 0.185 mm is observed from the simulation and can be seen in the lower plot. Therefore, at 6500 rpm engine speed the check valve and fuel injection system functions as required by not delivering the fuel during the exhaust event.

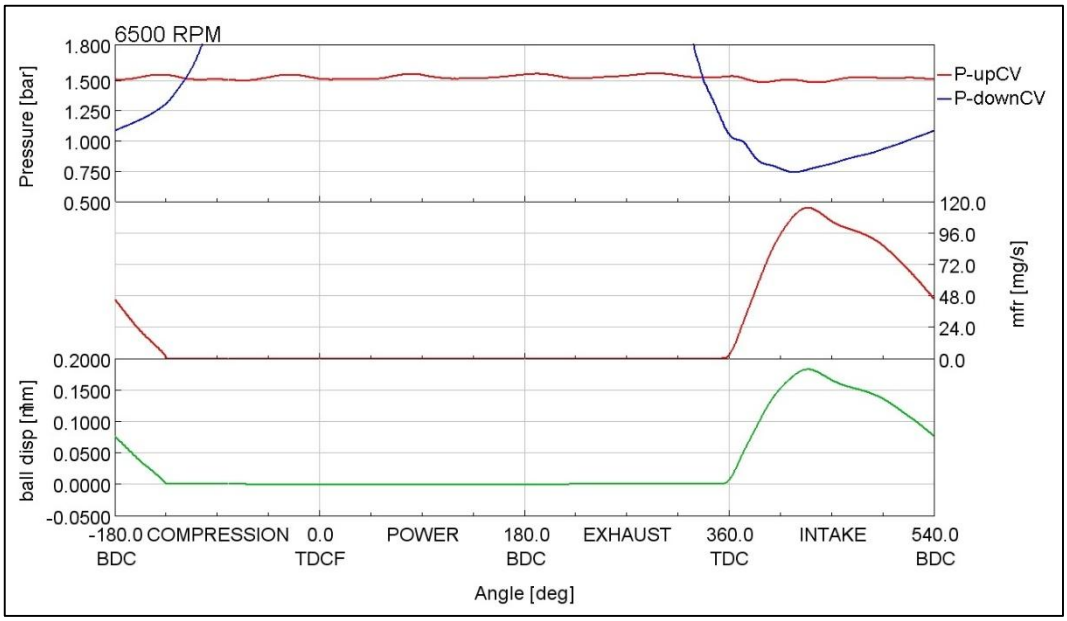

Figure 40 Pressure profile upstream and downstream the valve(upper plot), Instantaneous mass flow profile (middle plot), Ball displacement(lower plot) - Engine speed 6500 rpm

The upper plot in figure 41 represents the pressure profile during the engine operating speed of 3500 rpm. It can be observed that the downstream pressure of the check valve which is engine cylinder pressure shows fluctuations as compared to the previous case. A sudden rise in the cylinder pressure is observed at the end of the exhaust stroke. It is difficult to predict the reason behind it. The rise in the pressure could be caused by the late combustion of the unburnt fuel remaining in the cylinder or pressure oscillations in the exhaust manifold. CFD simulations can help us understand the results in a better way.

The middle plot shows us the fuel is delivered through the check valve during the exhaust stroke due to the fluctuations in the engine cylinder pressure due to exceeding the cracking pressure of the valve (approximately 31 kPa). The max ball displacement during the exhaust event is 0.20 mm which is twice the opening during the intake stroke.

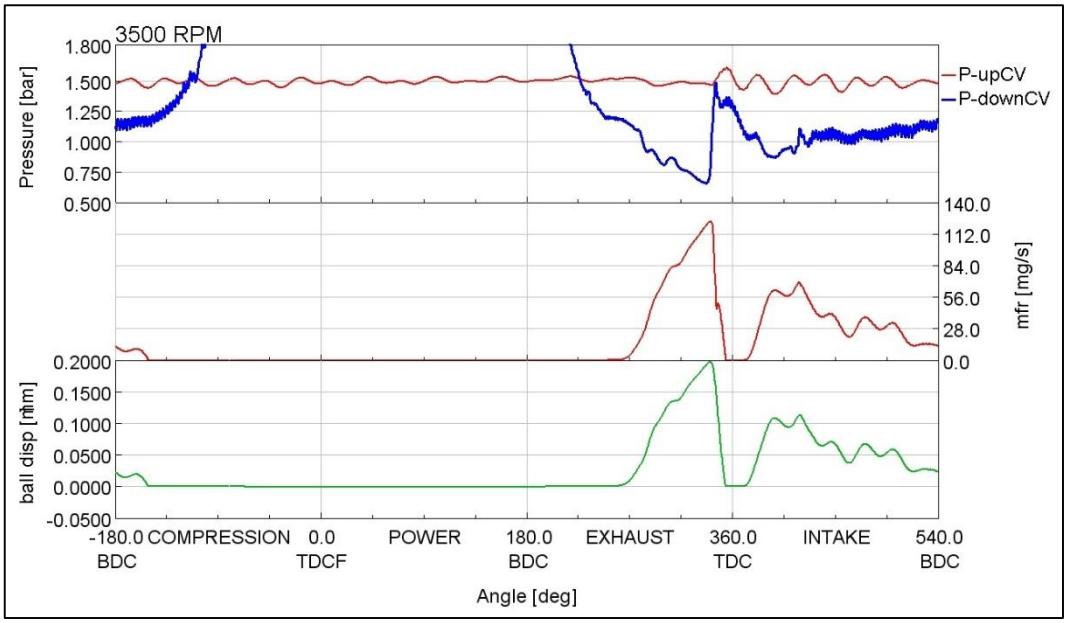

Figure 41 Pressure profile upstream and downstream the valve(upper plot), Instantaneous mass flow profile (middle plot), Ball displacement(lower plot) - Engine speed 3500 rpm

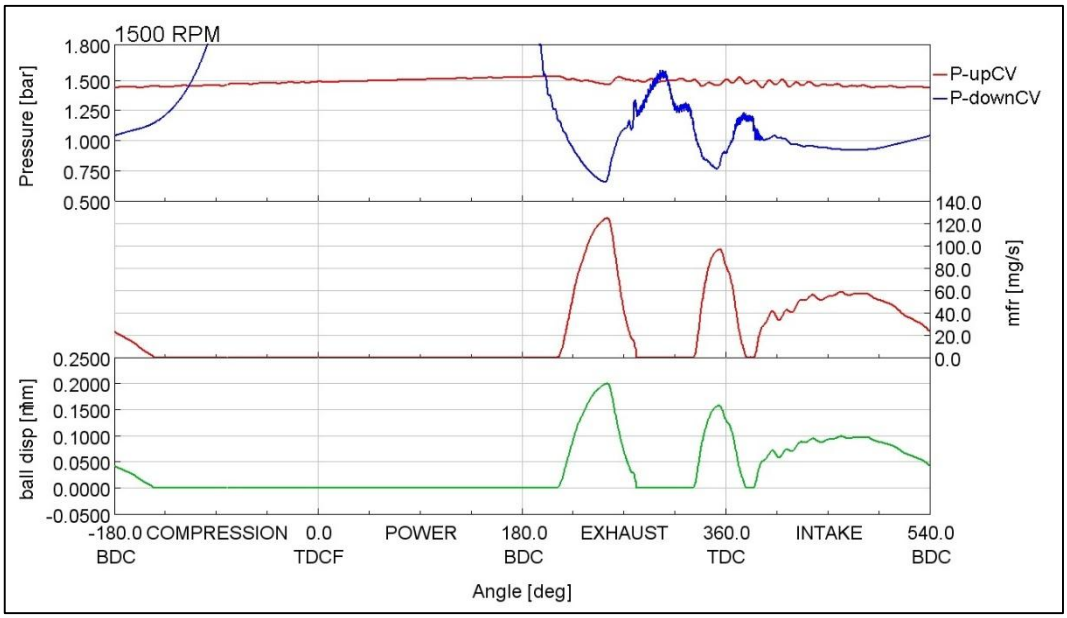

Figure 42 Pressure profile upstream and downstream the valve(upper plot), Instantaneous mass flow profile (middle plot), Ball displacement(lower plot) - Engine speed 1500 rpm

At an engine operating speed of 1500 rpm which can be idling speed of the engine, the pressure fluctuations in the engine cylinder are much greater than the engine operation at a relatively higher speed. Two pressure peaks are observed in the engine cylinder during the exhaust and intake stroke which can be seen in the upper plot of figure 42. Due to this pressure fluctuation, the fuel is delivered through the check valve

during the early exhaust stroke and a small amount at the end of the stroke. During the low-speed operation, the fuel losses are comparatively higher and which might increase the unburnt hydrocarbons emission. The fuel consumption will be higher at low operating speed.

The results for other engine operating speeds can be in the attachment A. It is noticed that as the speed reduces the injection of the fuel to the pre-chamber advances thus fuel losses are maximized.

6 Modal analysis of the Check Valve

A ball check valve is a simple non-return valve with spring and mass arrangement. The ball in the valve has a diameter of 2.1 mm. The ball is made up of structural steel and has a mass of 0.0378 grams. The spring which is elastic has the wire diameter of 0.1 mm and predicted stiffness from the studies is 0.44 N/mm.

All the systems possessing mass and elasticity are capable of free vibration. The system vibrates with some frequency which is termed as the natural frequency of the system. The displacement of the ball ie opening and closing of the valve which causes the fuel flow is dependent on the pressure difference of the valve which varies with the engine operation and its speed. The excitation of the ball valve depends on the external factors here it is pressure difference. The response of the system is non-periodic, The excitation duration depends on the engine speed. If the excitation frequency coincides with the natural frequency of the valve, the response will be large. This condition is called Resonance [23].

If the resonance condition will occur the system behavior will change and it might not deliver the fuel to the pre-chamber as required which will affect the performance of the engine. Thus it becomes important to find out the natural frequency of the system and compares it with the excitation frequency to check for resonance.

The excitation frequency here is the engine operating speed. When the engine is running at the highest speed of 6500 rpm, the excitation frequency is given by

$$\omega_e = \frac{2 * \pi * N}{60} = \frac{2 * \pi * 6500}{60} = 680.678\, rad/sec$$

$$\omega_e = 2 * \pi * f_e \quad \therefore \quad f_e = 108.38\, Hz$$

where,

N= Speed of engine

ω_e= Excitation frequency in rad/sec

f_e= Excitation frequency in Hertz (Hz)

The Natural frequency of the spring-mass system is given by [18]

$$w_n = \sqrt{\frac{k_s}{m}}$$

where,

w_n = Natural frequency of the check valve in rad/sec

f_n = Natural frequency of the check valve in Hertz (Hz)

k_s = Spring stiffness in N/m

m = mass of the ball in kg

$$w_n = \sqrt{\frac{k_s}{m}} = \sqrt{\frac{0.44 * 10^3}{0.0378 * 10^{-3}}} = 3411.77\ rad/sec$$

$$\omega_n = 2 * \pi * f_n \quad \therefore \quad f_n = 543\ Hz$$

The natural frequency of the check valve is 543 Hz and is 5 times higher than the excitation frequency of the system which is calculated at 6500 RPM. This proves there will bo any resonance condition and the check valve is safe for operation at high speed.

6.1 Natural frequencies of the spring

A helical spring with a diameter of 0.1 mm is used in the check valve. A spring that is elastic has its mass and thus will have natural frequencies. When the excitation frequency of the system coincides with the natural frequencies of the spring, resonance occurs. In this state, the spring is subjected to a wave of successive compression of the coils that travels from end to other and back. This type of vibratory motion is called a surge of the spring [24]. Generally, springs are designed in such a way that the natural frequency is 15 to 20 times more than excitation frequency to avoid resonance.

The natural frequencies of the spring are found out in the VTDESIGN workbench in GT SUITE. The input parameters given to the software are listed below. [25]

Parameter	Value	Units
Spring Stiffness	0.44	N/mm
Number of coils	9	

Coil diameter	0.1	mm
Wire cross-section	Circular	
Installed length	4	mm

Table 16 Design parameters of the spring

A force vs displacement characteristics plot was also an input to the workbench. The relation was obtained from steady-state results which shows the dependence of the ball lift with respect to the increasing pressure. The plot in the figure shows the characteristics of the spring.

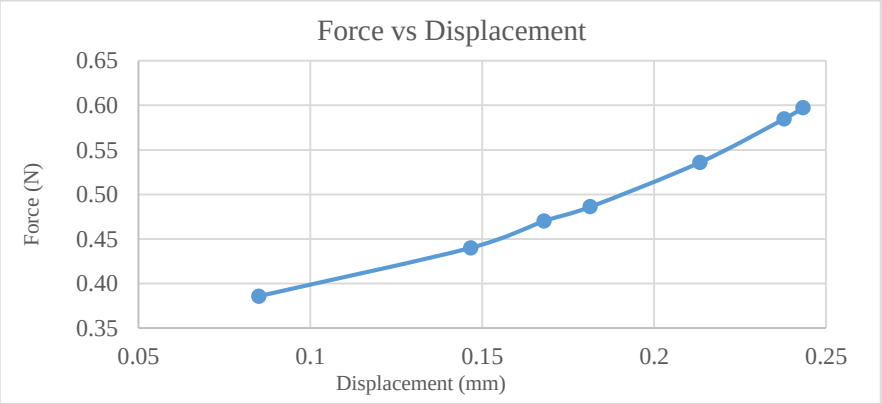

Figure 43 Force versus Displacement

Figure 41 shows the results from the VLDESIGN. The modal frequencies are calculated based on the geometry and other properties. An object can have infinite natural frequencies. For the spring, based on the data provided 17 mode shapes are calculated. The frequency of the first mode is 10 kHz which is 100 times more than the excitation frequency. Hence we can say no resonance will occur in the spring and it can function properly at high-speed engine operation.

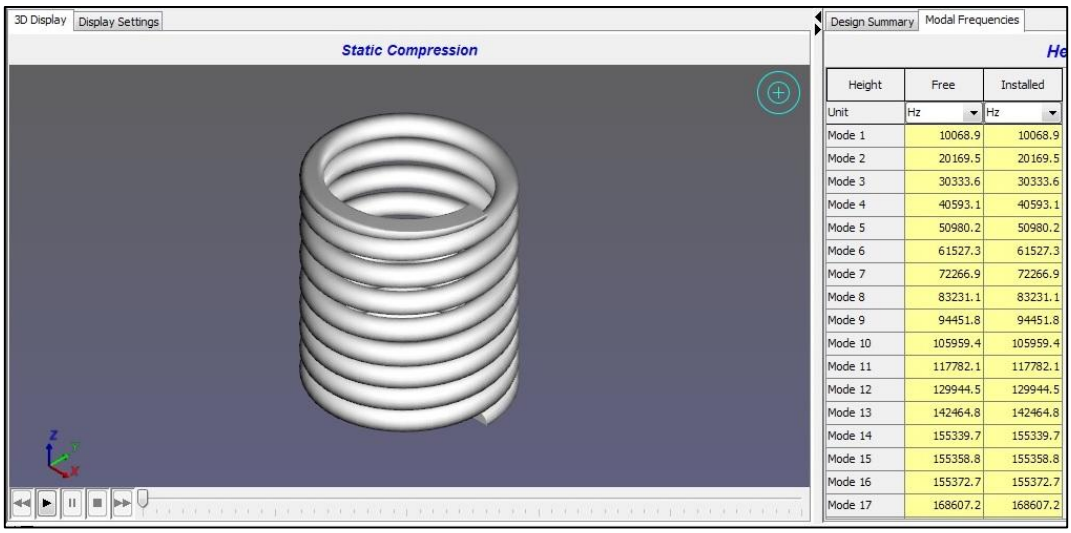

Height	Free	Installed
Unit	Hz	Hz
Mode 1	10068.9	10068.9
Mode 2	20169.5	20169.5
Mode 3	30333.6	30333.6
Mode 4	40593.1	40593.1
Mode 5	50980.2	50980.2
Mode 6	61527.3	61527.3
Mode 7	72266.9	72266.9
Mode 8	83231.1	83231.1
Mode 9	94451.8	94451.8
Mode 10	105959.4	105959.4
Mode 11	117782.1	117782.1
Mode 12	129944.5	129944.5
Mode 13	142464.8	142464.8
Mode 14	155339.7	155339.7
Mode 15	155358.8	155358.8
Mode 16	155372.7	155372.7
Mode 17	168607.2	168607.2

Figure 44 Modal frequencies of the Spring

Summary and Conclusion

Studies were conducted on the designed fuel injection system model in the GT model. The model was developed with the help of provided geometric data. The check valve being the most important part of the system was the main focus of the studies. Due to insufficient data on the mechanical parameters of the valve, it was difficult to analyze and study the behavior of it. For the mechanical parameters of the valve, we had to rely on the predicted value from the simulation.

Various simulations were carried out in GT Power to predicts the mechanical parameters of the valve. The degree of accuracy cannot be specified since there is no evidence for it. These mechanical parameters were helpful in further studies of the fuel injection system for high-speed engine operations. The model was calibrated for the flow rate passing through the check valve and using the methodology mentioned in section [4.2] the mechanical parameters were obtained. During the simulation, the fuel delivered through the check valve was also monitored.

Some key conclusions are as follows

i. The initial predicted mechanical parameters of the ball check valve are 0.44 N/mm spring stiffness and 31.79 kPa spring preload. However this parameters doesn't remain constant, it changes over the period.
ii. Spring preload is a very sensitive parameter and is affected the most, a significant drop in the preload from 31.79 kPa to 0.58 kPa was observed. The spring stiffness is also affected with change in the preload but the change is marginal.
iii. The flow rate passing through the check valve is dependent on the input fuel injection pressure to the pre-chamber. As the fuel injection pressure increases the fuel flowing through the check valve will increase.
iv. Change in the preload of the spring affects the cracking pressure of the valve. As the spring stiffness decreases, the flow rate tends to increase. [section 4.3]
v. Changes in the mechanical parameters of the check valve over the period due to operations, affect the flow rate passing through the check valve. Thus it becomes important to replace the check valve after a certain time or number of hours of the operation. Since the original application for the check valve is hydraulics. This information has to be provided by the engine durability tests.

vi. During the unsteady state engine operation, the fuel is delivered to the pre-chamber during the exhaust stroke of the cycle when the engine is operated up to 1800 rpm irrespective of the operating condition of the engine since the principle of opening and closing of the valve is pressure difference across it. This fuel doesn't take part in the main combustion event and may be accounted for the fuel loss. This fuel delivered during the exhaust stroke or at the end of power stroke might increase the unburnt hydrocarbons emissions or flow out during the exhaust stroke. Further studies will conclude it.

With the understanding of the behavior of the check valve, a new fuel injection system was developed with provided data and was integrated with a single-cylinder high-speed research engine model designed by the predecessors in GT Power. The aim was to see the performance of the check valve at higher operating speed of the engine at full load engine operation. No experimental tests are done on the high-speed engine setup currently. Therefore the current simulation results will help us understand how the fuel injection system to the pre-chamber is reacting to high-speed engine operation.

Following conclusion can be drawn from the results:

i. The principle of the fuel delivered to the pre-chamber is solely dependent on the difference between the fuel injection pressure and the pre-chamber pressure during the operation. No other parameter influence the opening and closing of the valve.
ii. At high-speed engine operation, the check valve delivers fuel to the pre-chamber at the exhaust stroke till early compression stroke, which is required.
iii. At engine speed below 3500 rpm, the fuel is delivered to the pre-chamber during early exhaust stroke which might be accounted as the fuel loss and must be verified by the experiments of CFD simulations
iv. During the idling speed, similar trends were observed, the fuel is delivered during the exhaust stroke of the engine, which might increase the unburnt hydrocarbon emission of the engine.

To avoid the fuel leak to the pre-chamber during the exhaust stroke, a control system has to be setup. A SOLENOID VALVE controlled by the ECU can be used upstream to the check valve. The valve will allow the fuel to flow towards the check valve only during the intake stroke event of the engine and remain closed during the other strokes.

The setting up of the control system to deliver the fuel to the pre-chamber as required is the future scope of the thesis. After setting up the controller, engine simulation can be carried out in the GT Power with the model already designed to study the performance of the engine. With the help of the simulation results, the experimental setup can be modified and engine testing can be done.

The model analysis of the check valve and its spring proves that there will be no resonance condition during the high-speed engine operation and the current check valve if used is safe for operations.

Future Scope of the thesis

- The current studies prove that the check valve is not solely sufficient to deliver the fuel to the pre-chamber as required. Therefore a control system has to be set up to control the flow.
- Setting up the control system in the GT suite for fuel control to the pre-chamber, simulating and studying the results
- Simulating the model for various operating conditions, current studies only shows the results for full load condition.
- Testing the experimental engine, comparison with the simulation results.

References

[1] „Rossman, The Effect of Vehicular Emissions on Human Health by Ronni Esther,“ [Online]. Available: http://teachers.yale.edu/curriculum/viewer/initiative_08.07.09_u.

[2] [Online]. Available: https://www.albert.io/learn/ap-environmental-science/global-warming--1/greenhouse-gases-global-warming-potential-and-emissions-by-sector/greenhouse-gases-most-influential-emissions?page=1.

[3] J. Vavra, Z. Syrovatka, M. Takats a E. Barrientos, „Scavenged Pre-chamber on a gas engine for light duty truck,“ *ASME 2016 Internal Combustion Fall Technical Conference,* č. ICEF2016-9423, 2016.

[4] C. Bach, T. Bütler a M. Huber, „Fuel consumption and emissions investigation on a passenger car, operated with natural gas - hydrogen mixtures,“ *Empa – Swiss Federal Laboratories for Materials Science and Technology, Internal Combustion Engines Laboratory, Ueberlandstrasse 129, CH-8600 Duebendorf* .

[5] A. Shah, „Improving the Efficiency of Gas Engines using Pre-chamber Ignition,“ Lund University, 2015.

[6] C. Dipl.-Ing Weber, U. Dr.-Ing Kramer, R. Dipl.-Ing Friedfeldt, H. Dr.-Ing Ruhland a F. Dr.-Ing Krämer, „Development of a New Combustion Engine Dedicated to Methane,“ Ford-Werke GmbH, , Köln, 2018.

[7] F. Ravet, G. Coma a P. Christou, „CNG direct injection spark-ignition engine with high turbulence and high compression ratio: numerical and experimental investigations,“ Powertrain and Vehicle Division IFP Energies nouvelles, Institut Carnot IFPEN Transports Energie Rond-point de l’échangeur de Solaize, BP 3, 69360 Solaize, France.

[8] „Reciprocating Engines: Emission Control PetroWiky.org,“ [Online]. Available: <http://petrowiki.org/Reciprocating-engines>.

[9] J. Heywood, Internal Combustion Engine Fundamentals, New York: McGraw-Hill, 1988.

[10] P. Soltic, T. Hilfike, S. Hänggi, R. Hutter a M. Weissner, „Ignition- and combustion concepts for lean operated passenger car natural gas engines," ETH Zürich, Institute for Dynamic Systems and Control CH-8092 Zürich.

[11] M. McMillian, S. Richardson a S. Woodruff, „Laser-Spark Ignition Testing in a Natural gas-fueled single-cylinder engine," *SAE TECHNICAL PAPER SERIES*, č. 2004-01-0980, 2004.

[12] [Online]. Available: https://contest.techbriefs.com/2014/entries/automotive-transportation/4259.

[13] G. Karim, „Combustion in Gas Fueled Compression: Ignition Engines of the dual-fuel type," *ASME. J. Eng. Gas Turbines Power,* Sv. %1 z %2125(3):827-836, 2003.

[14] United State Environmental Protection Agency, „ High-Authority Fuel Injection," 2001.

[15] H. Schock, E. Toulson a W. Attard, „A review of pre-chamber initiated jet ignition combustion systems," *SAE Technical Paper,* Sv. %1 z %22010-01-2263, č. 10.4271/2010-01-2263, 2010.

[16] H. R. Ricardo, „Internal-combusiton engine". US Patent Patent 1,271,942, 1918.

[17] [Online]. Available: http://www.diesel-rk.bmstu.ru/Eng/index.php?page=Vozmojnosti.

[18] Z. Syrovatka, M. Takats a J. Vavra, „Analysis of Scavenged Pre-Chamber for light-duty truck Gas engine," *SAE Technical Paper,* Sv. %1 z %22017-24-0095, 2017.

[19] M. ŠŤOURAL, „DP 2014 - SM06: Zapalovací komůrka pro plynový motor s nepřímým zážehem. Praha 2014,“ Diplomová práce. ČVUT v Praze Vedoucí práce Ing. Jiří Vávra, PhD..

[20] The LEE Company, *IMH Handbookof Hydraulics and Pnuematics*, 2016.

[21] G. S. Manuals.

[22] AVL, [Online]. Available: https://www.avl.com/documents/10138/885965/AVL+Pressure+Sensors+for+Combustion+Analysis/6c844a54-7a84-429d-8e57-4f34e948f95d.

[23] S. S. Rao, Mechanical Vibrations.

[24] K. Prof Gopinath a M. M. Prof Mayuram, Machine Design II.

[25] *GT Suite VTDESIGN.*

List of Figures

Figure 1 Green House Gases Emissions by sector [2] 4
Figure 2 Emissions versus air/fuel ratio [4] 6
Figure 3 Laser-Induced Ignition [7] 8
Figure 4 Pilot Injection [9] 9
Figure 5 First pre-chamber design by Riccardo 9
Figure 6 Working of the pre-chamber engine [12] 10
Figure 7 Scheme of current test engine layout 11
Figure 8 Pre-chamber Module Setup(left) and Cross-section of the cylinder head with pre-chamber assembly(right) 12
Figure 9 Pre-chamber geometry [13] 13
Figure 10 Ball check valve LEE 558 series forward flow 14
Figure 11 Laboratory fuel supply setup 17
Figure 12 Standard Volumetric flow rate (m^3/hr) versus Spring Stiffness(N/mm) . 19
Figure 13 Instantaneous mass flow profile (mg/sec) Ks=0.3 vs 0.5 vs 0.7 20
Figure 14 Standard Volumetric flow rate (m^3/hr) versus Spring preload(kPa) 21
Figure 15 Instantaneous mass flow profile (mg/sec) - Preload= 0 vs 7.5 vs 15.5 kPa 21
Figure 16 Volumetric flow rate(m^3/hr)- steady-state condition 23
Figure 17 Ball displacement(mm) - steady-state condition 23
Figure 18 Plot of Comparison of Volumetric flow rate(m^3/hr) versus input pressure(bar) between experimental data and simulation results 24
Figure 19 Ball displacement(mm) versus Input pressure(bar) 24
Figure 20 Plot of Comparison of Volumetric flow rate(m^3/hr) versus lambda between experimental data and simulation results - CASE 1 27
Figure 21 Results from the simulation, Pressure profile upstream and downstream of the valve(upper plot), instantaneous mass flow profile(middle plot), Integrated mass flow rate(lower plot)- lambda 0.98- CASE 1 27
Figure 22 Pressure profile upstream and downstream valve(upper plot), instantaneous mass flow profile(middle plot), integrated mass flow rate (lower plot) lambda 0.98 versus lambda 1.98- CASE 1 28
Figure 23 Plot of Volumetric flow rate(m^3/hr) versus input pressure(bar) comparison between experimental and simulation data - CASE 2 29
Figure 24 Instantaneous mass flow profile for one cycle(upper plot), Integrated mass flow rate (middle plot), Ball displacement in check valve(lower plot)-CASE 2 30
Figure 25 Plot of volumetric flow rate(m^3/hr) versus Engine speed(RPM) comparison between experimental and simulation results- CASE 3 31

Figure 26 Instantaneous mass flow profile for one cycle(upper plot), Standard volumetric flow rate (middle plot), Ball displacement in check valve(lower plot)- CASE 3 32
Figure 27 Pre-chamber pressure plot 33
Figure 28 Plot of Volumetric flow rate(m^3/hr) versus input pressure(bar) comparison between experimental and simulation data - CASE 4 34
Figure 29 Instantaneous mass flow profile(upper plot), Ball displacement(lower plot) – Pressure 1.16 vs 1.29 vs 1.45 35
Figure 30 Pressure upstream and downstream on the check valve at Pressure 1.45 bar 35
Figure 31 Specifications of the AVLGH15D pressure transducer [15] 36
Figure 32 Flame arrestor details [15] 36
Figure 33 Comparison between Cylinder pressure and pre-chamber pressure profile 37
Figure 34 Instantaneous mass flow profile (mg/sec) 38
Figure 35 Integrated mass flow rate(mg) 38
Figure 36 Pre-chamber for High-speed engine 42
Figure 37 Brake mean effective pressure(bar) vs engine speed (RPM) 44
Figure 38 BSFC (g/KW-hr) vs engine speed (RPM) 44
Figure 39 Fuel delivered through pre-chamber and injector 44
Figure 40 Pressure profile upstream and downstream the valve(upper plot), Instantaneous mass flow profile (middle plot), Ball displacement(lower plot) - Engine speed 6500 rpm 45
Figure 41 Pressure profile upstream and downstream the valve(upper plot), Instantaneous mass flow profile (middle plot), Ball displacement(lower plot) - Engine speed 3500 rpm 46
Figure 42 Pressure profile upstream and downstream the valve(upper plot), Instantaneous mass flow profile (middle plot), Ball displacement(lower plot) - Engine speed 1500 rpm 46
Figure 43 Force versus Displacement 50
Figure 44 Modal frequencies of the Spring 50

List of tables

Table 1 Main parameters of the Engine 12
Table 2 Pre-chamber parameters [3] 13
Table 3 Parameter that can be changed in the GT Power model 18
Table 4 Experimental and simulated data for the steady-state condition 22
Table 5 Predicted Mechanical Parameters- steady-state case 25
Table 6 Experimental and simulated data - Unsteady State condition- CASE 1 26
Table 7 Predicted Mechanical Parameters- unsteady state condition- CASE 1 27
Table 8 Experimental and simulated data - Unsteady-State condition- CASE 2 29
Table 9 Predicted Mechanical Parameters- unsteady state condition- CASE 2 30
Table 10 Experimental and simulated data - Unsteady State condition- CASE 3 31
Table 11 Predicted Mechanical Parameters- unsteady state condition- CASE 3 32
Table 12 Experimental and simulated data - Unsteady-State condition- CASE 4 33
Table 13 Predicted Mechanical Parameters- unsteady state condition- CASE 4 34
Table 14 Summary and comparison of predicted mechanical parameters 39
Table 15 Mechanical parameters of the check valve - LEE 588 series 41
Table 16 Design parameters of the spring 50

List of files attached in CD

- Final Thesis.pdf
- GT Power model- Fuel injection model
  - The engine in stationary condition(steady-state)
  - Unsteady state model
- GT Power model – Single Cylinder Research Engine model
- Calibration results for light-duty truck engine.xlsx

List of attachments

- Attachment A: Instantaneous pressure profile and mass flow profile for different speeds- Full load operation
- Attachment B: LEE ball check valve – 558 Series
- Attachment C: Schematic of the fuel supply to the pre-chamber
- Attachment D: Fuel Injection system model
- Attachment F: High-speed engine model with integrated fueling system to the pre-chamber

Attachment A: Instantaneous pressure profile and mass flow profile for different speeds

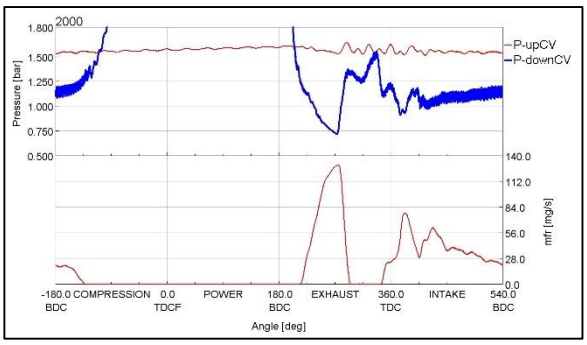

Speed – 2000 rpm

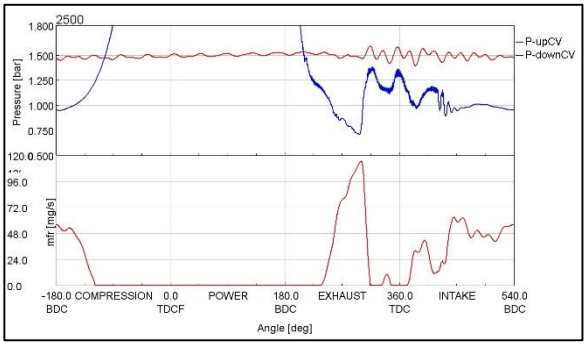

Speed – 2500 rpm

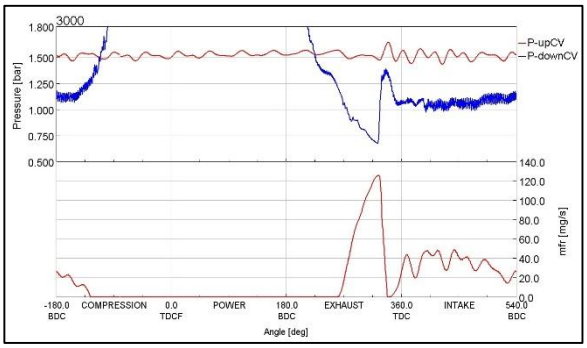

Speed – 3000 rpm

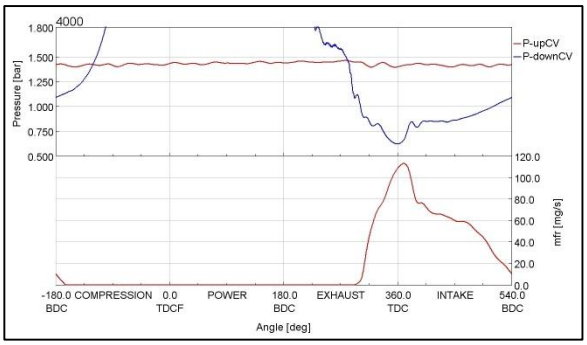

Speed – 4000 rpm

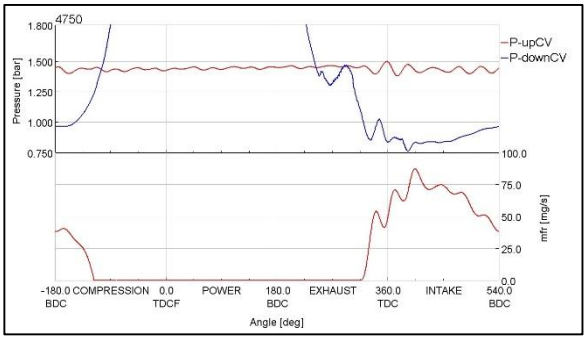

Speed – 4750 rpm

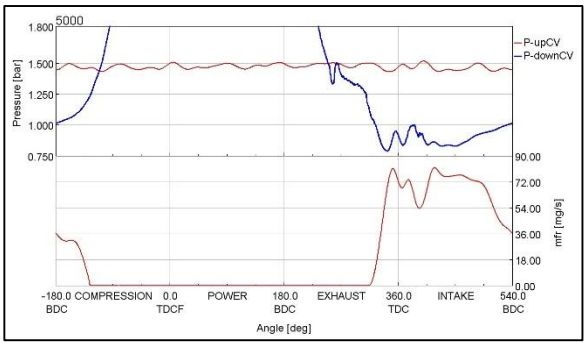

Speed – 5000 rpm

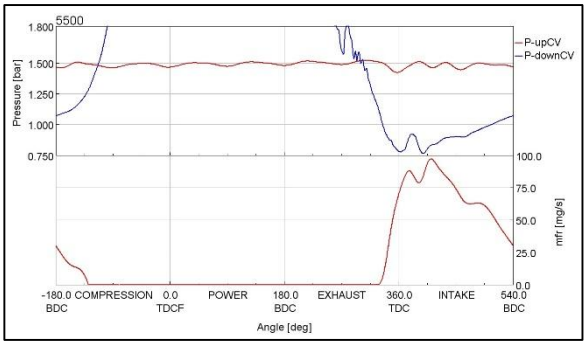

Speed – 5500 rpm

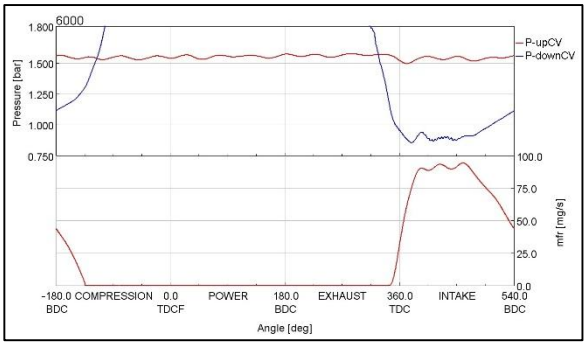

Speed – 6000 rpm

Attachment B- LEE ball check valve – 558 Series

INSERT CHECK VALVES

A6

558 SERIES CHEK VALVE - FORWARD FLOW

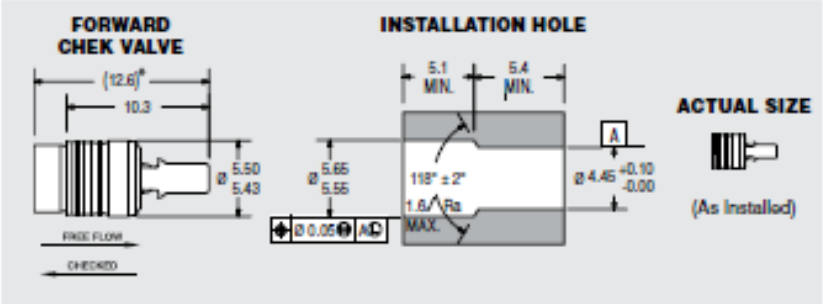

* *LOA before installation.*
All dimensions in millimeters.

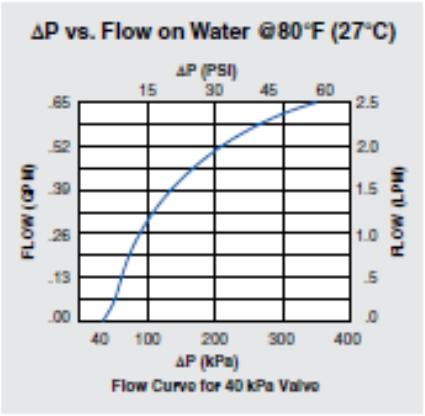

LEE PART NO.	CRACKING PRESSURE
CCFM2550200S	0 kPa (No Spring)
CCFM2550204S	4 ± 3 kPa (0.6 ± 0.4 psid)
CCFM2550207S	7 ± 5 kPa (1 ± 0.7 psid)
CCFM2550214S	14 ± 5 kPa (2 ± 0.7 psid)
CCFM2550225S	25 ± 10 kPa (3.6 ± 1.5 psid)
CCFM2550240S	40 ± 30 kPa (6 ± 4.4 psid)
CCFM2550269S	69 ± 17 kPa (10 ± 2.5 psid)

PERFORMANCE

Lohm Rate: 250 Lohms

Leakage: 20 sccm/min. (max.) @ 172 kPa (25 psid) on air

1 Drop/min. (max.) on hydraulic fluid

Maximum Working Pressure:
28 MPa (4,060 psid)
(Checked Direction)

4 MPa (580 psid)
(Flow Direction)

MATERIALS

Body ..... 303 Stainless Steel
Cage ..... 305 Stainless Steel
Pin ..... 416 Stainless Steel
Spring ..... 302 Stainless Steel
Ball ..... 440C Stainless Steel

INSTALLATION

Tool Part Number CCRT0900120S
Force ..... 625 Kg F (max.)
For Installation procedure see page A1.

Attachment C: Schematic of the fuel supply to the pre-chamber

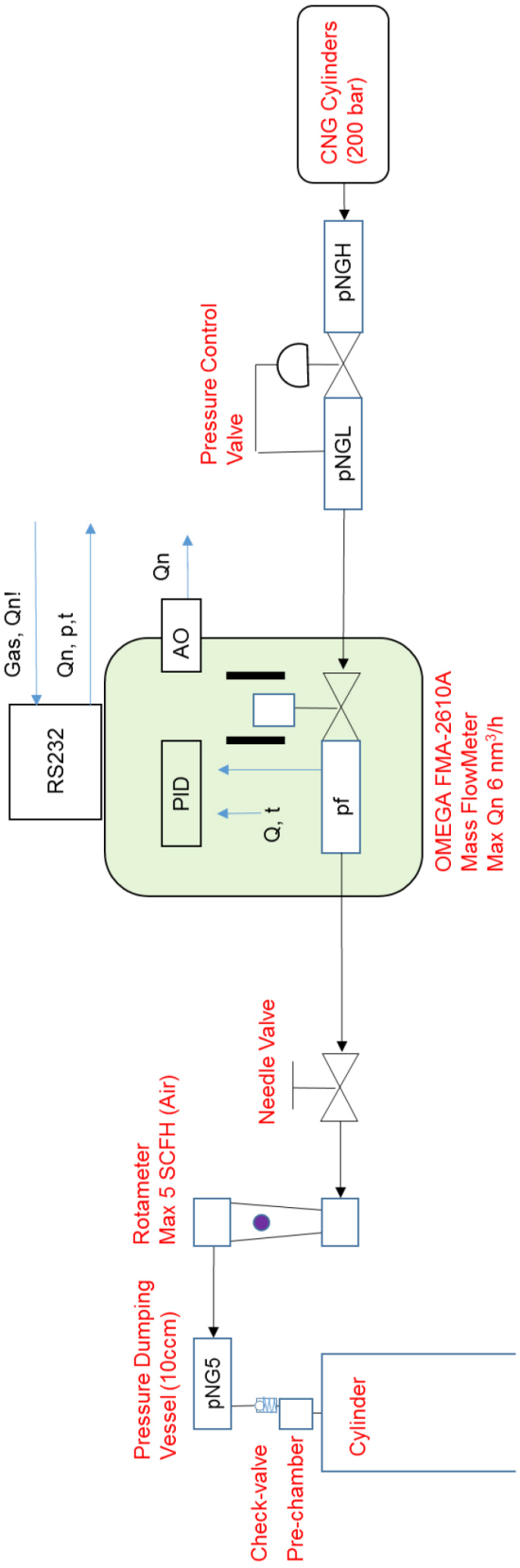

Attachment D – Fuel Injection system model

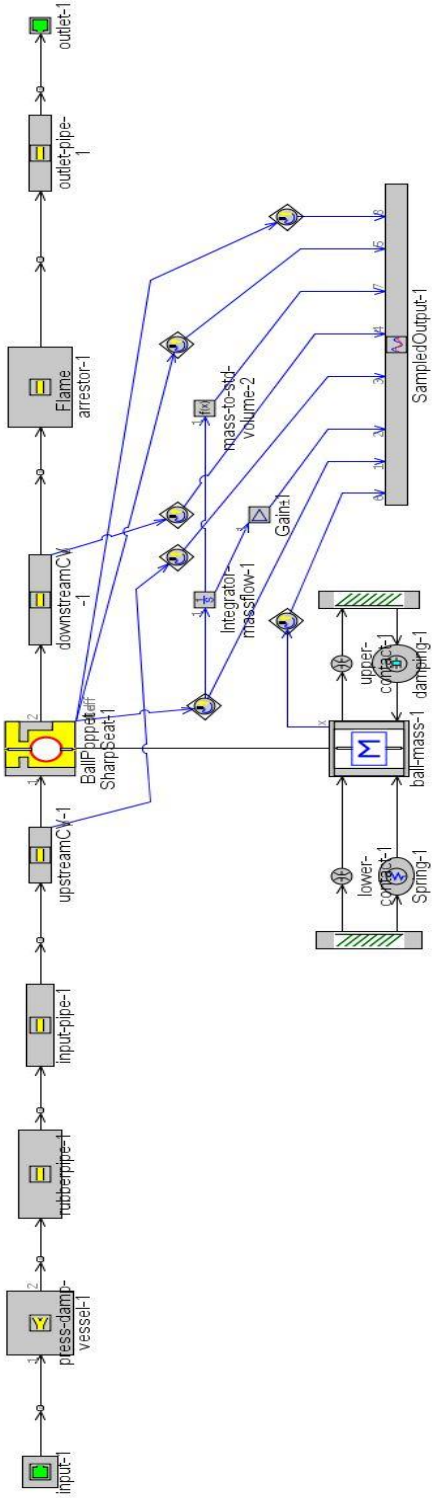

Attachment E – High-speed engine model with integrated fueling system to the pre-chamber